

NSWC/WOL TR 78-189

LEVEL

12
B.S.

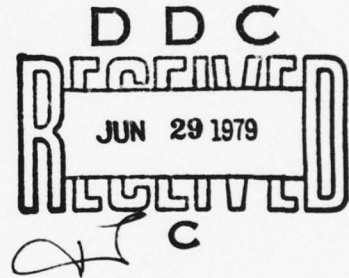
AD A 070 571

**OBSERVATIONS ON PARACHUTE SCALE FACTORS FOR
MODELING PARACHUTE DEPLOYMENT AND STEADY
STATE PERFORMANCE**

BY WILLIAM P. LUDTKE

UNDERWATER SYSTEMS DEPARTMENT

9 MAY 1979



Approved for public release, distribution unlimited.

DDC FILE COPY.



NAVAL SURFACE WEAPONS CENTER

Dahlgren, Virginia 22448 • Silver Spring, Maryland 20910

79 06 28 007.

UNCLASSIFIED

SECURITY CLASSIFICATION OF THIS PAGE (When Data Entered)

REPORT DOCUMENTATION PAGE		READ INSTRUCTIONS BEFORE COMPLETING FORM	
1. REPORT NUMBER 14 NSWC/WOL/ TR-78-189 ✓	2. GOVT ACCESSION NO.	3. RECIPIENT'S CATALOG NUMBER 9 (rept. for)	4. TYPE OF REPORT & PERIOD COVERED Final FY 78
5. TITLE (and Subtitle) 6 OBSERVATIONS ON PARACHUTE SCALE FACTORS FOR MODELING PARACHUTE DEPLOYMENT AND STEADY STATE PERFORMANCE		6. PERFORMING ORG. REPORT NUMBER	
7. AUTHOR(s) 10 William P./Ludtke		8. CONTRACT OR GRANT NUMBER(s)	
9. PERFORMING ORGANIZATION NAME AND ADDRESS Naval Surface Weapons Center ✓ White Oak, Silver Spring, Maryland 20910		10. PROGRAM ELEMENT, PROJECT, TASK AREA & WORK UNIT NUMBERS 0; 12 65A	
11. CONTROLLING OFFICE NAME AND ADDRESS		12. REPORT DATE 11 9 May 1979	
14. MONITORING AGENCY NAME & ADDRESS (if different from Controlling Office)		13. NUMBER OF PAGES 65	
		15. SECURITY CLASS. (of this report) UNCLASSIFIED	
		15a. DECLASSIFICATION/DOWNGRADING SCHEDULE	
16. DISTRIBUTION STATEMENT (of this Report) Approved for public release, distribution unlimited			
17. DISTRIBUTION STATEMENT (of the abstract entered in Block 20, if different from Report)			
18. SUPPLEMENTARY NOTES			
19. KEY WORDS (Continue on reverse side if necessary and identify by block number) Parachute scaling effects; mass ratio; parachute opening shock; Reynolds number; characteristic length for parachutes; initial area at deployment.			
20. ABSTRACT (Continue on reverse side if necessary and identify by block number) A new approach to the scaling of parachute performance is presented, based upon variables inherent in the inflation process such as weight, time, geometry, etc. Limitations of conventional scaling parameters such as Reynold's, Froude, and Mach numbers as applied to parachutes are discussed. Examples of parachute inflation and steady state performance are correlated with a scale factor designated as a Mass Ratio, which is the ratio of the system mass to a mass of atmosphere associated with the parachute size, inflation time, altitude and deployment velocity. For advanced opening shock analyses, the concept of			

DD FORM 1473

JAN 73

EDITION OF 1 NOV 65 IS OBSOLETE
S/N 0102-LF-014-6601

UNCLASSIFIED

SECURITY CLASSIFICATION OF THIS PAGE (When Data Entered)

391 596


J03

UNCLASSIFIED

SECURITY CLASSIFICATION OF THIS PAGE (When Data Entered)

ABSTRACT (Block 20) (Cont'd)

variable mass ratio during canopy inflation is proposed, and the effects of partial canopy inflation at suspension line stretch are discussed. Although the solid cloth types of parachutes are primarily used as examples, the ideas of mass ratio, initial area, and analysis techniques are applicable to all types of parachutes.



UNCLASSIFIED

SECURITY CLASSIFICATION OF THIS PAGE (When Data Entered)

SUMMARY

The investigation presented in this report is related to the improvement of parachute technology.

V.C.D. Dawson

V.C.D. DAWSON
By direction

Accession For	
NTIS GMA&I	<input checked="checked" type="checkbox"/>
DDC TAB	<input type="checkbox"/>
Unannounced	<input type="checkbox"/>
Justification	
By	
Distribution/	
Availability Codes	
Dist	Avail and/or special
<i>A</i>	

CONTENTS

	Page
INTRODUCTION	7
DEVELOPMENT OF THE MASS RATIO CONCEPT	7
MASS RATIO APPLICATION TO DEPLOYING SOLID CLOTH PARACHUTES . .	14
CONCLUSIONS	19
APPENDIX A DISCUSSION OF CHARACTERISTIC LENGTH	A-1
APPENDIX B A TECHNIQUE FOR THE CALCULATION OF THE OPENING- SHOCK FORCES FOR SEVERAL TYPES OF SOLID CLOTH PARACHUTES	B-1
APPENDIX C A GUIDE FOR THE USE OF APPENDIX B	C-1
APPENDIX D EFFECT OF INITIAL AREA RATIO ON THE LIMITING MASS RATIO FOR THE FINITE STATE OF SOLID CLOTH PARACHUTE DEPLOYMENT	D-1
LIST OF SYMBOLS	S-1
GLOSSARY OF TERMS	G-1

ILLUSTRATIONS

<u>Figure</u>		<u>Page</u>
1	Retarded Automobile	9
2	Visualization of the Mass Ratio Concept	10
3	Variation of Affected Air Mass Along a Fully Inflated Parachute Trajectory	11
4	Variation of Scale Factors with Time for Example 1	13
5	Comparison of the Variation of Ballistic Coefficient and Mass Ratio During the Unfolding Phase of Solid Cloth Parachute Deployment	16
6	Comparison of Affected Air Volumes for Single Value and Variable Mass Ratios	18
7	Dependency of Mass Ratio and Reference Time on Parachute Geometry, Air Flow Properties, Drag Area Signature, and Deployment Conditions for Solid Cloth Parachutes	20
(Appendix B)		
1	Typical Infinite Mass Force-Time History of a Solid Cloth Parachute in a Wind Tunnel	B-2
2	Typical Force-Time Curve for a Solid Flat Parachute Under Infinite Mass Conditions	B-2
3	Typical Force-Time Curve for a 10% Extended Skirt Parachute Under Infinite Mass Conditions	B-2
4	Typical Force-Time Curve for a Personnel Guide Surface Parachute Under Infinite Mass Conditions	B-2
5	Typical Force-Time Signature for the Elliptical Parachute Under Infinite Mass Conditions	B-2
6	Typical Force-Time Signature for the Ring Slot Parachute 20% Geometric Porosity Under Infinite Mass Conditions	B-2
7	Drag Area Ratio Vs. Time Ratio	B-3
8	Visualization of the Mass Ratio Concept	B-3
9	Effect of Initial Area and Mass Ratio on the Shock Factor and Velocity Ratio During the Unfolding Phase for $\eta = 0$	B-5
10	Effect of Initial Area and Mass Ratio on the Shock Factor and Velocity Ratio During the Unfolding Phase for $\eta = 0.2$	B-5
11	Partially Inflated Parachute Canopy	B-6
12	Effect of Altitude on the Unfolding Time " t_0 " At Constant Dynamic Pressure for $\eta = 1/2$ and $\eta = 0.63296$	B-7
13	Effect of Altitude on the Unfolding Distance At Constant Velocity and Constant Dynamic Pressure for $\eta = 1/2$ and $\eta = 0.63246$	B-7

ILLUSTRATIONS (Cont'd)

<u>Figure</u>		<u>Page</u>
(Appendix B)		
14	Variation of Steady-State Drag, F_s , and Maximum Opening Shock with Altitude for Constant Velocity and Constant Dynamic Pressure	B-7
15	Maximum Drag Area Ratio Vs. Initial Elongation	B-9
16	Nominal Porosity of Parachute Material Vs Differential Pressure	B-10
17	Comparison of Measured and Calculated Permeability for Relatively Permeable and Impermeable Cloths	B-11
18	Effect of Pressure Coefficient and Altitude on the Unfolding Time	B-11
19	The Effective Porosity of Parachute Materials Vs. Differential Pressure	B-11
20	Effect of Altitude on Mass Flow Ratio At Constant Velocity	B-12
21	Effect of Velocity on Mass Flow Ratio At Constant Velocity	B-12
22	Location of Data Points for Determination of "k" and "n"	B-12
23	Airflow Patterns Showing Air Volume Ahead of Canopy Hem	B-13
24	Parachute Cross Section Nomenclature	B-13
D-1	Effect of Initial Area Ratio on the Limiting Mass Ratio for the Finite State of Parachute Deployment for Solid Cloth Parachutes	D-3
D-2	Variation of the Finite Mass Shock Factor During the Unfolding Phase of Solid Cloth Parachutes for Limiting Mass Ratios and Initial Area Effects	D-4

INTRODUCTION

The author has been actively engaged in applied research, design, manufacture, and testing of parachutes and parachute systems since 1952. In this period many improvements have been accomplished in the prediction of parachute opening shock performance and trajectory analysis. The coming of age of the computer was a blessing in that it permitted detailed modeling of parachute deployments, but, at the same time, in many cases, it reduced the need to understand some of the underlying basics of the parachute deployment process. One of those basics is a scale factor parameter. The development of the scale factor element is fundamental to the understanding of parachute performance. This paper is a presentation of the author's current ideas and reasoning on what is required to permit establishment of a means of scaling parachute deployments and trajectories. A discussion of what variables are required and examples of existing application and proposed method of application are offered. This will be accomplished by first developing the mass ratio quantity by use of a horizontal trajectory with a fully deployed parachute. The concept will then be extended to show applicability to inflating parachutes, and, finally, methods for including the mass ratio as a variable in the canopy inflation process are suggested. This paper is presented with the purpose that the thoughts expressed may assist and stimulate other experimentors in the development of future advanced analysis techniques.

DEVELOPMENT OF THE MASS RATIO CONCEPT

In model testing of airplanes, missiles, ships, etc. in wind tunnels and towing basins, Reynold's number, Froude number, and Mach number are accepted scale factors. These parameters, together with ballistic coefficient ($W/C_D S_0$) and surface loading (W/S_0), have not provided a general correlation of parachute test data. A viable scaling parameter for general use in deployable decelerator testing has not been developed, although some experimentors have successfully modeled particular cases. A look at the methods of testing gives us a clue as to why the aforementioned scale factors do not apply to parachute deployment. In the testing of airplanes, missiles, ships, etc., a rigid model is constructed and mounted in the wind tunnel, towing basin, etc., and data recorded at one or more constant velocities. Thus, three parameters which are important to parachute

testing are eliminated. First, the geometry of a deploying parachute undergoes dramatic changes as compared to the constant geometry of the rigid model. Second, the deploying parachute geometry is a function of deployment time. Third, the velocity profile obtained during a parachute deployment is dependent upon the mass of the assembly being retarded. Transient geometry, time, and weight are not factors in the aforementioned scale parameters. This leads to some very important conclusions:

a. Reynold's number, Froude number, and Mach number are valid scale factors for airplanes, missiles, ships, etc., because they contain the variables which affect performance.

b. These established scale parameters are unsuitable for parachute deployments because they do not contain important variables which affect parachute performance.

c. For any quantity to be a valid scale parameter in any process, it must contain those variables which affect system performance.

An example of a "mass ratio" ratio scale factor can be developed in a theoretical horizontal point mass trajectory. For simplicity, only the steady state (constant drag area, $C_D S_0$) will be considered; however, it will later be demonstrated that the developed mass ratio is also applicable for parachute deployments.

Example 1: Determine the velocity profile of an automobile which is being retarded on a horizontal road by a fully deployed parachute. Assume negligible automobile aerodynamic drag and road friction forces.

With reference to Figure 1,

$$-F = ma$$

$$F = \frac{1}{2} \rho V^2 C_D S_0$$

$$-\frac{1}{2} \rho V^2 C_D S_0 = \frac{W}{g} \frac{dV}{dt}$$

$$\frac{\rho g C_D S_0}{2W} \int_0^t dt = \int_{V_s}^V \frac{-dV}{V^2}$$

Integrating and solving for the velocity ratio

$$\frac{V}{V_s} = \frac{1}{1 + \frac{\rho g V_s t C_D S_0}{2W}} \quad (1)$$

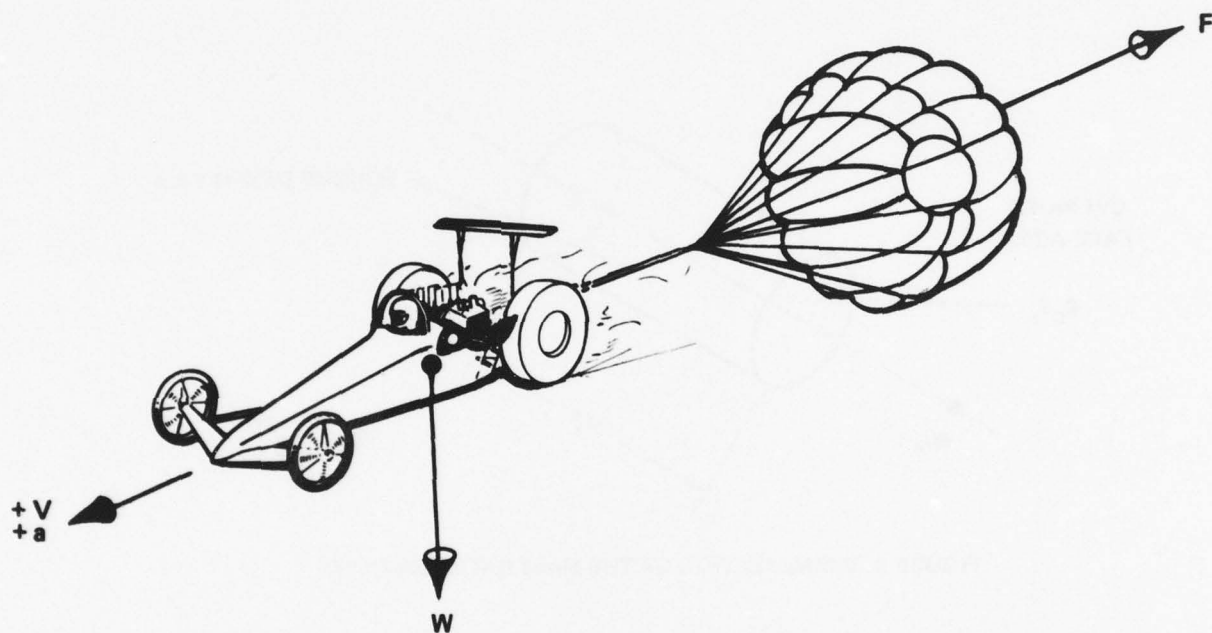


FIGURE 1 RETARDED AUTOMOBILE
SEE EXAMPLE 1

The quantity $2W/\rho g V_s t C_D S_0$ is in effect a mass ratio. It can be visualized as in Figure 2 to be the ratio of the mass of the system, W/g , to the mass of air contained in a right circular cylinder of face area $C_D S_0$, length $V_s t$, and mass density ρ . If this quantity is denoted by M , then Equation (1) becomes

$$\frac{V}{V_s} = \frac{1}{1 + \frac{1}{M}} \quad (2)$$

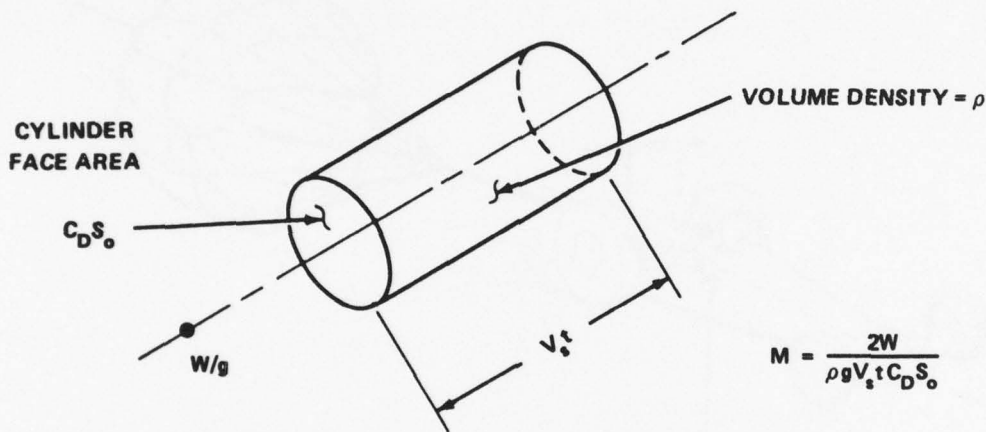


FIGURE 2 VISUALIZATION OF THE MASS RATIO CONCEPT

Figure 3 illustrates the concept of how the air mass is affected as the automobile moves along the retarded trajectory. As time increases, additional air mass is affected, and at each instant, a definite velocity ratio and mass ratio exist, as shown in Equation (2). Note that the length $V_s t$ in Figure 3 is not a true trajectory distance because of the use of the constant initial velocity V_s for all times. This mass ratio contains the basic variables (altitude, ρ ; parachute aerodynamic size, $C_D S_0$; system mass, W/g ; velocity, V_s ; and time) necessary to define a scale factor for deployable decelerator application. Apparent mass is another effect which should probably be included, but is not presently sufficiently understood or defined as to permit inclusion in the analysis.

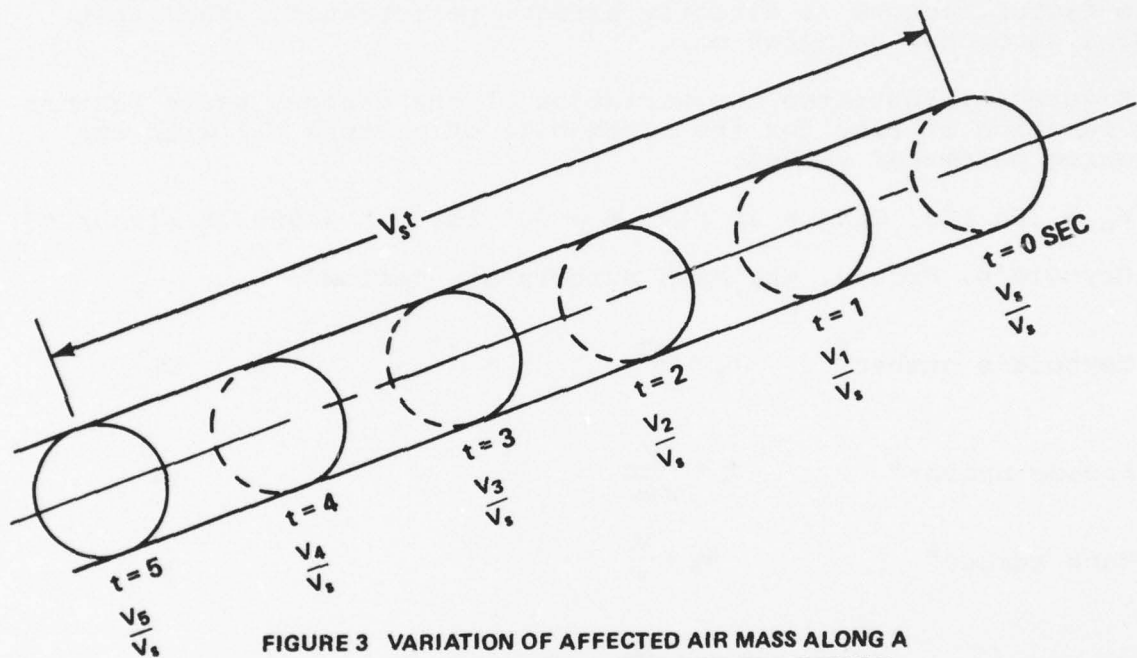


FIGURE 3 VARIATION OF AFFECTED AIR MASS ALONG A FULLY INFLATED PARACHUTE TRAJECTORY

As the automobile is retarded, the Reynold's, Froude, and Mach numbers vary along the trajectory as the velocity ratio changes. For the steady-state trajectory, only the ballistic coefficient, $W/C_D S_0$, remains constant throughout the trajectory and can be used as indicative of performance. If Reynold's, Froude, or Mach numbers are to be considered, the question becomes which of the many numbers should be used. From Equation (2) the velocity ratio can be determined for any time, t , into the trajectory. Once the velocity is known, the Reynold's, Froude, and Mach numbers can be determined. However, before these three scale factors could be computed, the mass ratio had to be calculated first in order to obtain the velocity ratio. Therefore, the mass ratio, even though it also varies along the trajectory, once again is the superior scale factor because it directly affects performance rather than being a secondary calculation.

Figure 4 illustrates the variation of the various scale factors as a function of time for the automobile of example (1) with the following parameter values:

$$V_s = 300 \text{ fps}, C_D S_0 = 25 \text{ ft}^2, W = 500 \text{ lb}, \rho = 0.002378 \text{ slugs/ft}^3.$$

The Reynold's, Froude, and Mach numbers are defined:

$$\text{Reynold's number}^* \quad R_e = \frac{\rho V L}{\mu} \quad (3)$$

$$\text{Froude number}^* \quad F_r = \frac{V}{\sqrt{g L}} \quad (4)$$

$$\text{Mach number}^* \quad M_n = \frac{V}{c} \quad (5)$$

$$\text{The Mass Ratio} \quad M = \frac{2W}{\rho g V_s t C_D S_0} \quad (6)$$

Some of the mass ratio variables appear in each of the preceding scale factors. Then it is possible to express the mass ratio M as some function of (R_e, F_r, M_n) . The only limitation is that a single value of $V=V_s$ be used.

$$\text{From Equation (3)} \quad \frac{1}{\rho V_s} = \frac{L}{\mu R_e}$$

* The characteristic length, L , in Reynold's and Froude numbers is taken as the square root of the drag area. For a discussion of characteristic length, see Appendix A.

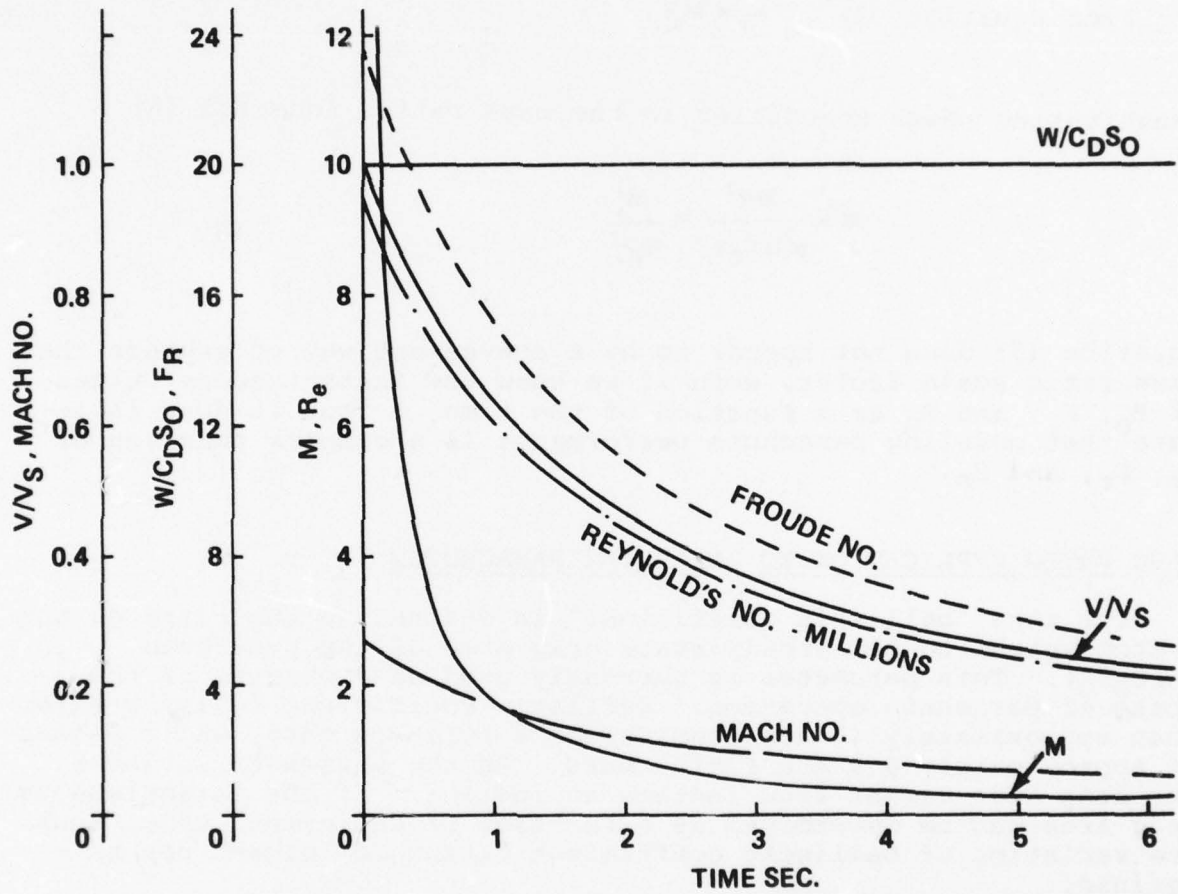


FIGURE 4 VARIATION OF SCALE FACTORS WITH TIME FOR EXAMPLE 1

From Equation (4)
$$L = \frac{V_s^2}{g F_r^2}$$

Therefore,
$$\frac{1}{\rho V_s} = \frac{V_s^2}{g \mu F_r^2 R_e}$$

From Equation (5)
$$V_s = M_n c$$

Substituting these quantities in the mass ratio, Equation (6)

$$M = \frac{2Wc^2}{g^2 t \mu C_D S_0} \times \frac{M_n^2}{R_e F_r^2} \quad (7)$$

Equation (7) does not appear to be a convenient way to express the mass ratio scale factor, even if we knew the instantaneous values of R_e , F_r , and M_n as a function of the time, t , but it does indicate that modeling parachute performance is a complex function of R_e , F_r , and M_n .

MASS RATIO APPLICATION TO DEPLOYING PARACHUTES

The term "ballistic coefficient" is defined as the ratio of the system weight to the steady-state drag area of the parachute ($W/C_D S_0$). This parameter is currently used as a measure of the state of parachute operation. Ballistic coefficient values greater than approximately 40 are considered as infinite mass, while values of approximately 0.3 are finite mass. As the parachute inflates, the drag area varies from instant to instant. If the instantaneous drag area can be determined as a function of deployment time, then the variation of ballistic coefficient during deployment can be defined.

Appendix B develops an empirical deployment drag area ratio expression for specified solid cloth types of parachutes as a function of deployment time ratio, which is expressed in Equation (8).

$$\frac{C_D S}{C_D S_0} = \left[(1 - \eta) \left(\frac{t}{t_0} \right)^3 + \eta \right]^2 \quad (8)$$

The development of this expression is a very important concept because it demonstrates that the parachute geometry variation during deployment is independent of altitude and velocity and is only dependent upon the initial geometry (η) and the deployment time ratio. Berndt, in Reference 1, confirmed this proposition by testing parachute systems at various altitudes and velocities.

For the convenience of the reader, the paper in which Equation (8) was developed is included as Appendix B. A guide for the use of Appendix B is included as Appendix C. When the instantaneous drag area ($C_D S$) in the transient ballistic coefficient (B.C.), Equation (9), is replaced by Equation (8), the variation of the ballistic coefficient during deployment is shown to be:

$$\text{B.C.} = \frac{W}{C_D S} \quad (9)$$

$$\text{B.C.} = \frac{W}{C_{D0} S_0 \left[(1 - \eta) \left(\frac{t}{t_0} \right)^3 + \eta \right]^2} \quad (10)$$

When the initial condition, η , approaches zero, the ballistic coefficient approaches infinity at time $t=0$. From this initial value, the ballistic coefficient then modifies from instant to instant to whatever final ballistic coefficient ($W/C_{D0} S_0$) (infinite mass, intermediate mass, or finite mass) the particular system under study possesses. For any given value of $W/C_{D0} S_0$ and η , the variation during deployment is always the same (see Fig. 5).

Appendix B developed a mass ratio scale factor similar to Equation (6) for an inflating solid cloth parachute, which was a constant value throughout the deployment process. The only difference between the mass ratio of Appendix B and the mass ratio visualized in Figure 2 is that the variable time t is replaced by the discrete time t_0 .

The magnitude of the mass ratio (M) together with the initial area effect (η) determine the state of parachute operation

1. Berndt, R.J. and DeWeese, J.H., "Filling Time Prediction Approach for Solid Cloth Type Parachute Canopies," AIAA Aerodynamic Decelerations Systems Conference, Houston, Texas, 7-9 Sep 1966.

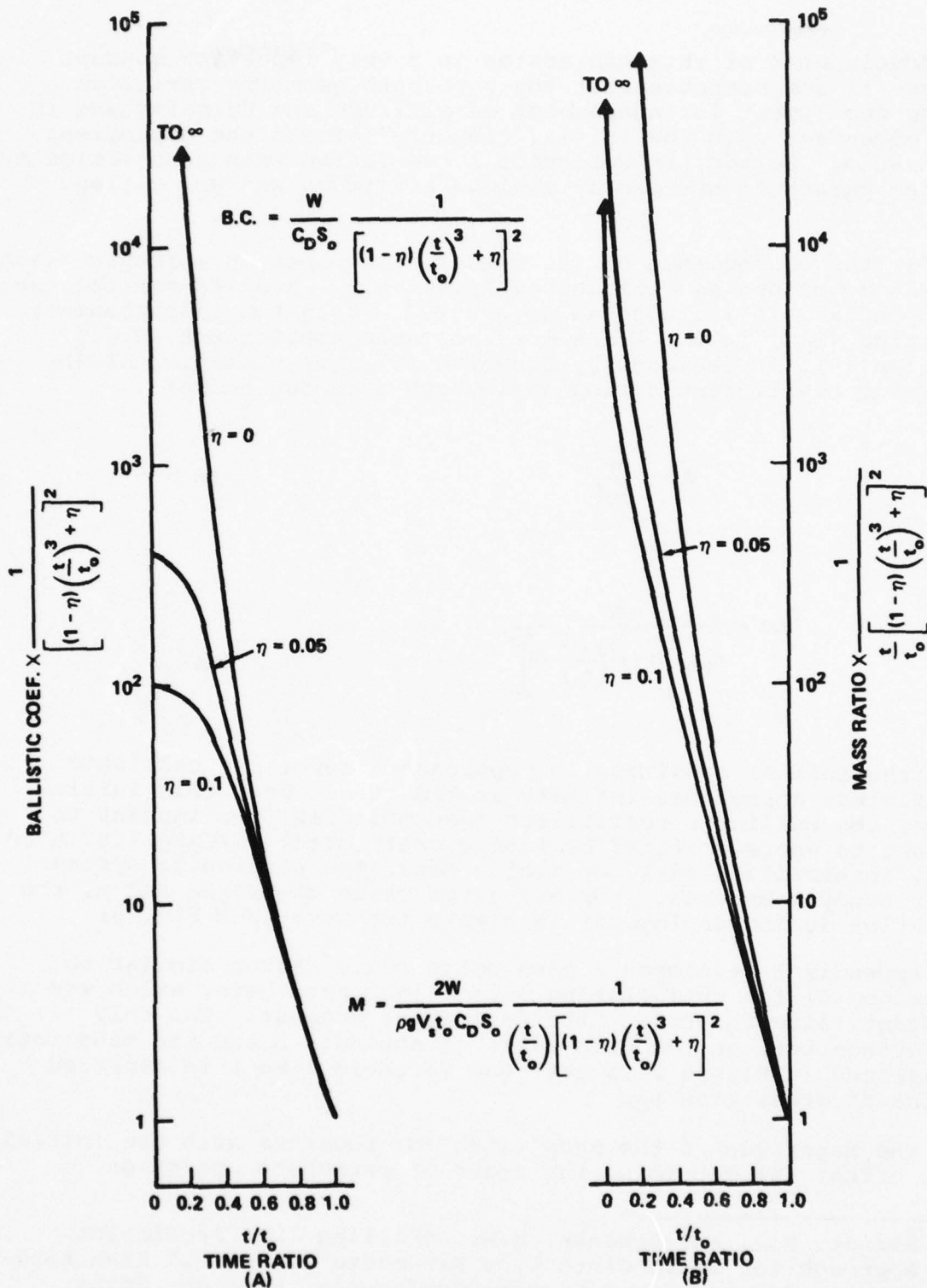


FIGURE 5 COMPARISON OF THE VARIATION OF BALLISTIC COEFFICIENT AND MASS RATIO DURING THE UNFOLDING PHASE OF SOLID CLOTH PARACHUTE DEPLOYMENT

(infinite mass, etc.), the velocity ratios during deployment, the maximum opening shock force, and the time of occurrence of the maximum shock during or after the unfolding phase of deployment. Examination of Figures 9 and 10, p. B-5, Appendix B, discloses that in this system of measurement mass ratios greater than 10 are essentially infinite mass state of deployment, and for $\eta=0$ mass ratios less than 0.19 are finite mass state of deployment. In between these limits are intermediate mass ratio values where the parachute opening shock occurs after time t_0 , but can be significantly less than infinite mass calculations. The mass ratio limit for the finite state of deployment is dependent on the value of η . An analysis of limiting mass ratios is presented in Appendix D.

In the method of developing the inflating parachute analysis, only one value of mass ratio was possible. The concept of a non-constant mass ratio during inflation was an innovation which occurred after the publication of Appendix B. A possible development of variable mass ratio during canopy inflation requires that the reference time t_0 and the steady-state drag area $C_D S_0$ be replaced by their variable counterparts t and $C_D S$.

$$M = \frac{2W}{\rho g V_s t C_D S}$$

When $C_D S$ is defined by Equation (8) and the denominator is multiplied by $t_0/t_0=1$.

$$M = \frac{2W}{\rho g V_s t_0 C_D S_0 \left(\frac{t}{t_0}\right) \left[(1-\eta) \left(\frac{t}{t_0}\right)^3 + \eta \right]^2} \quad (11)$$

The mass ratio, unlike the ballistic coefficient, is infinite for all values of η at the beginning of deployment. The variations of mass ratio during deployment is compared to the variation of ballistic coefficient as a function of η in Figure 5.

A comparison of the development of the affected air volumes for single value and variable mass ratios is visualized in Figure 6. The variable mass ratio air volume, as shown, is for a mass ratio greater than the limiting value. In the method of calculation in Appendix B, the elasticity of the materials are not considered significant in finite mass deployments, because the maximum opening shock occurs before full inflation.

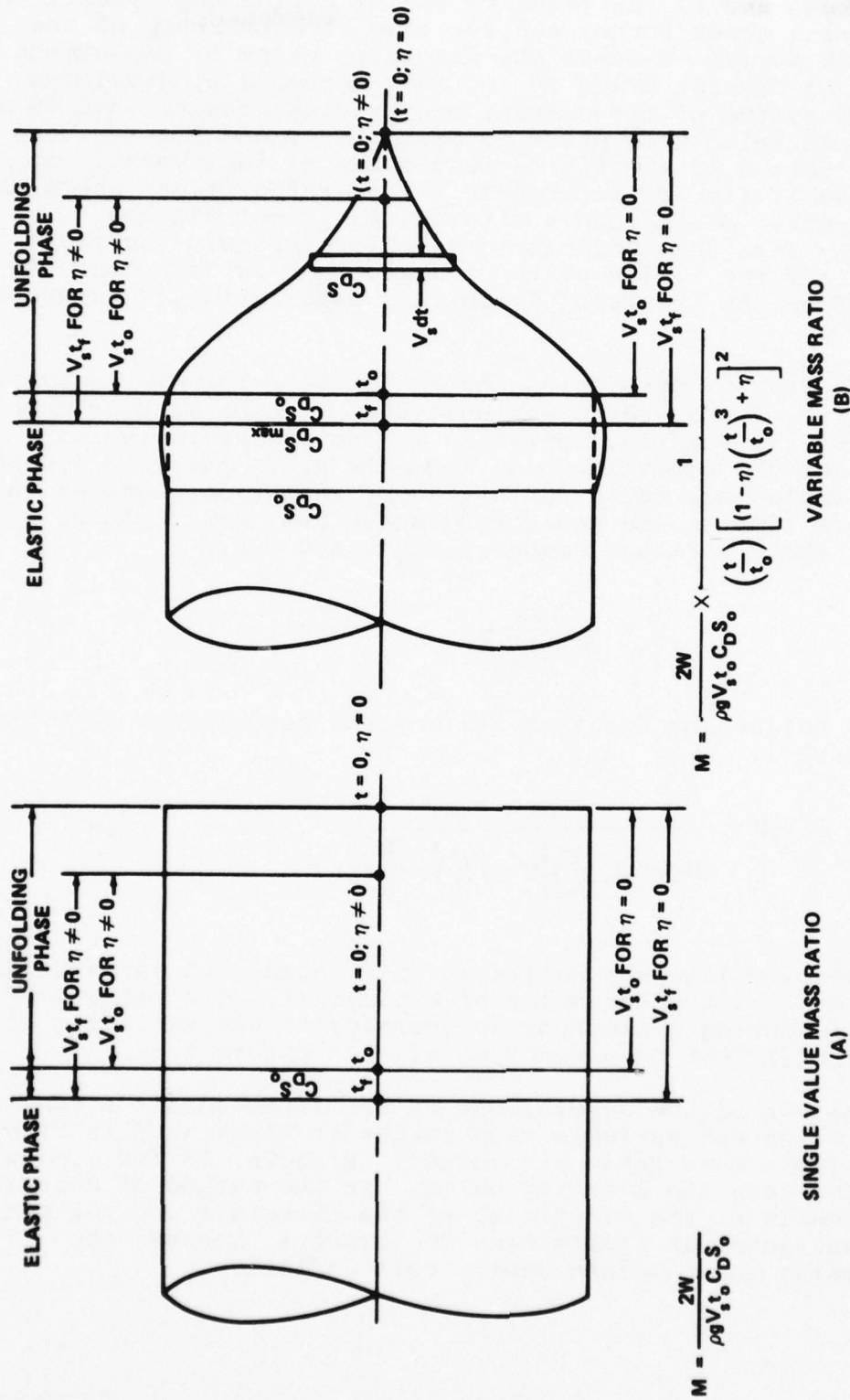


FIGURE 6 COMPARISON OF AFFECTED AIR VOLUMES FOR SINGLE VALUE AND VARIABLE MASS RATIOS

CONCLUSIONS

The following conclusions are derived from the arguments presented in this paper.

1. Scale factors for use in parachute performance analysis must contain those variables which affect operation. Weight, time, variable geometry, and air flow through the canopy are very important parameters not accounted for by Reynold's, Froude, and Mach number similitude expressions. The mass ratio, M , which does contain the basic parameters required for a meaningful scale factor, was derived from the analysis of a horizontal retarded trajectory. The visualization of Equation (6), in Figure 2, when viewed in this manner, demonstrates that this quantity is a true ratio of masses, while Equation (2) and Figure 3 show that the trajectory performance is dependent upon the affected air mass as a function of time.

2. Scale factors for parachutes are likely to be complicated functions of Reynold's, Froude, and Mach numbers. An improvement in the application of Reynold's number and Froude number to parachutes can be attained by utilizing a characteristic length whose magnitude is equal to the square root of the steady-state drag area. This reference length provides a logical basis for comparing the retarded fully inflated parachute trajectories for any type of parachute for a single value of Reynold's number. At the same time, canopy deployments for parachutes of differing inflation characteristics will vary for identical Reynold's number or Froude number.

New names were applied to the steady-state drag area and the characteristic length. These names are "Aerodynamic Size" and "Aerodynamic Diameter," respectively.

3. The realization that the geometry of parachute deployment is independent of altitude, velocity, and system mass is a very important discovery! The deployment geometry can now be separated from the forces generated and analyzed separately. Drag area signatures obtained from infinite mass wind tunnel tests are applicable to finite mass and intermediate mass analysis.

4. The mass ratio equation, M , is the same for all types of parachutes. When different types of parachutes are tested under identical deployment conditions, the particular mass ratio for a given parachute type is dependent upon the reference time t_0 . The reference time t_0 is dependent upon the geometry, air flow properties of the canopy, drag area signature, and deployment conditions. For the solid cloth types of parachutes of Appendix B, the dependency of the mass ratio and reference time on the aforementioned parameters are illustrated in the flow chart of Figure 7. The technique of Appendix B can be used to develop an analysis for other types of parachutes, once the inflation drag

W = SYSTEM WEIGHT, LB
 ρ = DENSITY AT DEPLOYMENT ALTITUDE, SLUGS/FT³
 V_s = SYSTEM VELOCITY AT SUSPENSION LINE STRETCH, FPS
 t_o = REFERENCE TIME OF UNFOLDING PHASE OF CANOPY INFLATION, SEC
 $C_D S_o$ = SYSTEM STEADY STATE DRAG AREA, FT²
 g = GRAVITY, FT/SEC²
 P = CANOPY CLOTH PERMEABILITY, FT³/FT²/SEC
 V_o = STEADY STATE CANOPY VOLUME, FT³
 A_{Mo} = STEADY STATE MOUTH AREA, FT²
 A_{so} = CANOPY SURFACE AREA, FT²
 $\frac{C_D S}{C_D S_o}$ = DRAG AREA SIGNATURE
 η = INITIAL AREA
 t/t_o = DEPLOYMENT TIME RATIO
 k & n = CLOTH AIR FLOW CONSTANTS
 C_p = CANOPY PRESSURE COEFFICIENT
 V = INSTANTANEOUS TRAJECTORY VELOCITY, FPS

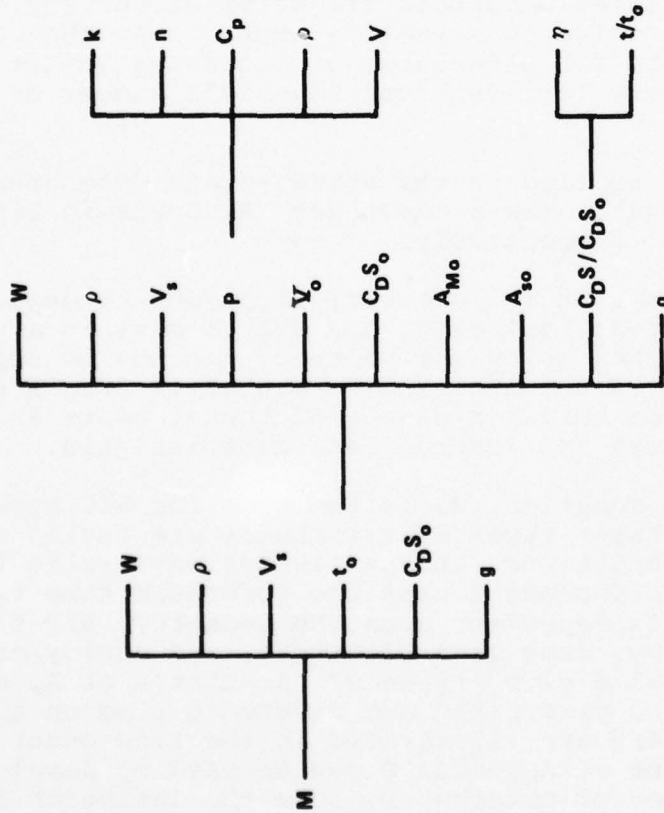


FIGURE 7 DEPENDENCE OF MASS RATIO AND REFERENCE TIME
 ON PARACHUTE GEOMETRY, AIR FLOW PROPERTIES,
 DRAG AREA SIGNATURE, AND DEPLOYMENT
 CONDITIONS FOR SOLID CLOTH PARACHUTES

area signature has been determined as a function of initial area and deployment time ratio from infinite mass wind tunnel deployments and methods of handling airflow through the canopy are developed. Treating the drag area as a single quantity as opposed to instantaneous drag coefficients and areas simplifies the problem and appears to be adequate for calculating forces.

5. The mass ratio concept from the horizontal trajectory analysis was applied to the inflation analysis of several types of solid cloth parachutes of Appendix B. A single value of mass ratio was used throughout the inflation process, and reasonable results were obtained. In addition, the effects of altitude on inflation distance and shock factor were analytically described.

6. As a further advance in inflation analysis, the idea of a variable mass ratio during canopy inflation was introduced. For both ballistic coefficient and mass ratio approaches, it was demonstrated that all inflation processes begin as infinite mass quantities. Future analysis of opening shock which utilizes a variable mass ratio during deployment should improve the accuracy of the analysis as it more nearly approaches the realistic environment.

7. The initial area of the parachute at suspension line stretch is dependent upon the deployment system for magnitude and repeatability. The effects of η on deployment forces can be evaluated by treating η as a variable and calculating the resulting forces for constant deployment conditions.

As η increases, the reference time t_0 is reduced with a subsequent rise in the mass ratio and shock factor. In finite mass deployments, the increase in parachute drag force early in inflation reduces the maximum force at $t = t_0$. The amount of reduction depends upon the mass ratio. At a value of approximately $\eta = 0.4$, the shock factors at $t = 0$ and $t = t_0$ are essentially equal (see Fig. D-2). Initial area ratios of this magnitude can be adapted to the deployment analysis of the second stage of a reefed parachute by considering the disreefing as the deployment of a parachute with a large η .

8. As the mass ratio increases during finite deployment, the maximum force occurs later in the inflation process. The mass ratio which causes the maximum force to occur at $t = t_0$ is defined as the limiting mass ratio, M_L , which is a function of η .

Appendix A

DISCUSSION OF CHARACTERISTIC LENGTH

The application of Reynold's number and Froude number to the scaling of parachute performance is not satisfactory. One cause of this deficiency is the definition of the characteristic length used in each of these parameters. Many experimenters quote values of Reynold's number per foot of length, regardless of the geometric size of the parachute, in order to avoid the necessity of defining a characteristic length.

If a wide range of any given type of parachute sizes were tested at constant deployment conditions and attached mass, the opening shock characteristics and the inflight trajectories vary for each of the parachute sizes used, but the Reynold's number per foot remains constant. This is illogical. It could be argued in this case that use of the parachute design diameter, D_0 , would suffice as a characteristic length because the various trajectories are different by reason of the different canopy sizes. Where this argument breaks down is when a different type of parachute of the same design drag area ($C_D S_0$) is substituted, such as a ribbon type of canopy being substituted for a solid flat canopy. In this case the inflight trajectories are matched, but the geometric diameter of the ribbon chute is considerably larger than the equivalent flat circular. The use of the geometric diameter in this case would give two values of Reynold's number for the same inflight trajectory. The "best choice" of reference length is that length which will define the inflight trajectories for similar ballistic coefficients ($W/C_D S_0$) by one value of Reynold's number. The characteristic length described in Equation (A-1) meets the single value criteria.

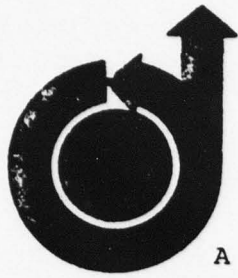
$$L = D_A = \sqrt{C_D S_0} \quad (A-1)$$

The opening shock force characteristics of the different types of parachutes will vary for identical Reynold's numbers. The fact that the deployment performance of various types of parachutes is different for identical Reynold's numbers is to be expected and logical.

The following proposals are offered:

a. The characteristic length used in Reynold's number calculations as applied to parachutes be defined as per Equation (A-1) and be named the "Aerodynamic Diameter." The aerodynamic diameter shall be designated by the symbol " D_A ."

b. If we consider the surface area (S_O) of a parachute as related to the geometric size of the canopy, then in the same manner the drag area ($C_D S_O$) can be related to the designation "Aerodynamic Size."



NSWC/WOL TR 78-189

Appendix B

A TECHNIQUE FOR THE CALCULATION OF THE
OPENING-SHOCK FORCES FOR SEVERAL
TYPES OF SOLID CLOTH PARACHUTES

**AIAA Paper
No. 73-477**

A TECHNIQUE FOR THE CALCULATION OF THE
OPENING-SHOCK FORCES FOR SEVERAL TYPES OF
SOLID CLOTH PARACHUTES

by
W. P. LUDTKE
Naval Ordnance Laboratory
Silver Spring, Maryland

AIAA 4th Aerodynamic Deceleration Systems Conference

PALM SPRINGS, CALIFORNIA / MAY 21-23, 1973

First publication rights reserved by American Institute of Aeronautics and Astronautics.
1290 Avenue of the Americas, New York, N. Y. 10019. Abstracts may be published without
permission if credit is given to author and to AIAA. (Price: AIAA Member \$1.50. Nonmember \$2.00).

Note: This paper available at AIAA New York office for six months;
thereafter, photoprint copies are available at photocopy prices from
AIAA Library, 750 3rd Avenue, New York, New York 10017

A TECHNIQUE FOR THE CALCULATION OF THE OPENING-SHOCK FORCES FOR SEVERAL TYPES OF SOLID CLOTH PARACHUTES

W. P. Ludtke
Naval Ordnance Laboratory
Silver Spring, Maryland

Abstract

An analytical method of calculating parachute opening-shock forces based upon wind-tunnel derived drag area time signatures of several solid cloth parachute types in conjunction with a scale factor and retardation system steady-state parameters has been developed. Methods of analyzing the inflation time, geometry, cloth airflow properties and materials elasticity are included. The effects of mass ratio and altitude on the magnitude and time of occurrence of the maximum opening shock are consistent with observed field test phenomena.

I. Introduction

In 1965, the Naval Ordnance Laboratory (NOL) was engaged in a project which utilized a 35-foot-diameter, 10-percent extended-skirt parachute (type T-10) as the second stage of a retardation system for a 250-pound payload. Deployment of the T-10 parachute was to be accomplished at an altitude of 100,000 feet. In this rarefied atmosphere, the problem was to determine the second stage deployment conditions for successful operation. A search of available field test information indicated a lack of data on the use of solid cloth parachutes at altitudes above 30,000 feet.

The approach to this problem was as follows: Utilizing existing wind-tunnel data, low-altitude field test data, and reasonable assumptions, a unique engineering approach to the inflation time and opening-shock problem was evolved that provided satisfactory results. Basically, the method combines a wind-tunnel derived drag area ratio signature as a function of deployment time with a scale factor and Newton's second law of motion to analyze the velocity and force profiles during deployment. The parachute deployment sequence is divided into two phases. The first phase, called "unfolding phase," where the canopy is undergoing changes in shape, is considered to be inelastic as the parachute inflates initially to its steady-state aerodynamic size for the first time. At this point, the "elastic phase" is entered where it is considered that the elasticity of the parachute materials enters the problem and resists the applied forces until the canopy has reached full inflation.

The developed equations are in agreement with the observed performance of solid cloth parachutes in the field, such as the decrease of inflation time as

altitude increases, effects of altitude on opening-shock force, finite and infinite mass operation, and inflation distance.

II. Development of Velocity Ratio and Force Ratio Equations During the Unfolding Phase of Parachute Deployment

The parachute deployment would take place in a horizontal attitude in accordance with Newton's second law of motion.

$$\Sigma F = ma$$

$$-\frac{1}{2} \rho v^2 C_D S = \frac{W}{g} \frac{dv}{dt}$$

It was recognized that other factors, such as included air mass, apparent mass, and their derivatives, also contribute forces acting on the system. Since definition of these parameters was difficult, the analysis was conducted in the simplified form shown above. Comparison of calculated results and test results indicated that the omitted terms have a small effect.

$$\int_0^t C_D S dt = \frac{-2W}{\rho g} \int_{V_s}^V \frac{dv}{v^2} \quad (1)$$

Multiplying the right-hand side of equation (1) by

$$1 = \frac{V_s t_o C_D S_o}{V_s t_o C_D S_o}$$

and rearranging

$$\begin{aligned} \frac{1}{t_o} \int_0^t \frac{C_D S}{C_D S_o} dt \\ = \frac{-2W}{\rho g V_s t_o C_D S_o} V_s \int_{V_s}^V \frac{dv}{v^2} \end{aligned} \quad (2)$$

In order to integrate the left-hand term of equation (2), the drag area ratio must be defined for the type of parachute under

analysis as a function of deployment reference time, t_0 .

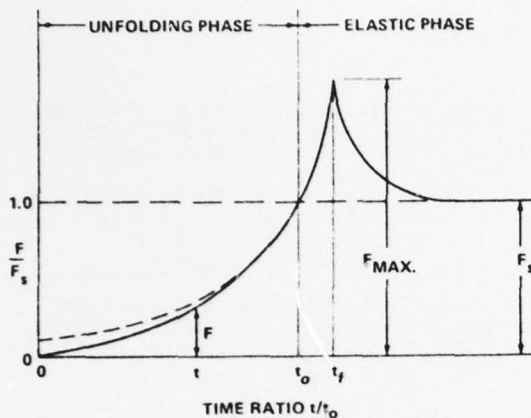


FIG. 1 TYPICAL INFINITE MASS FORCE-TIME HISTORY OF A SOLID CLOTH PARACHUTE IN A WIND TUNNEL

Figure 1 illustrates a typical solid cloth parachute wind-tunnel infinite mass force-time history after snatch. In infinite mass deployment, the maximum size and maximum shock force occur at the time of full inflation, t_f . However, t_f is inappropriate for analysis since it is dependent upon the applied load, structural strength, and materials elasticity. The reference time, t_0 , where the parachute has attained its steady-state aerodynamic size for the first time, is used as the basis for performance calculations.

At any instant during the unfolding phase, the force ratio F/F_s can be determined as a function of the time ratio, t/t_0 .

$$F = \frac{1}{2} \rho v^2 C_D S$$

$$F_s = \frac{1}{2} \rho v_s^2 C_D S_0$$

Since the wind-tunnel velocity and density are constant during infinite mass deployment

$$\frac{F}{F_s} = \frac{C_D S}{C_D S_0}$$

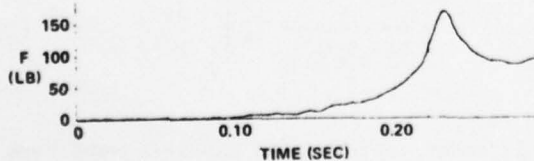
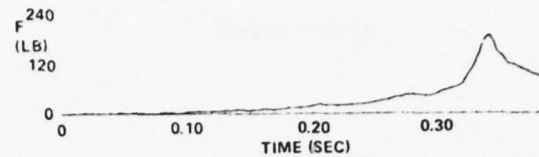
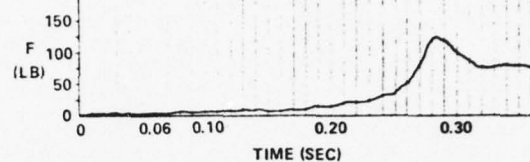


FIG. 2 TYPICAL FORCE-TIME CURVE FOR A SOLID FLAT PARACHUTE UNDER INFINITE MASS CONDITIONS.



REPRODUCED FROM REFERENCE (1)

FIG. 3 TYPICAL FORCE-TIME CURVE FOR A 10% EXTENDED SKIRT PARACHUTE UNDER INFINITE MASS CONDITIONS.



REPRODUCED FROM REFERENCE (1)

FIG. 4 TYPICAL FORCE-TIME CURVE FOR A PERSONNEL GUIDE SURFACE PARACHUTE UNDER INFINITE MASS CONDITIONS

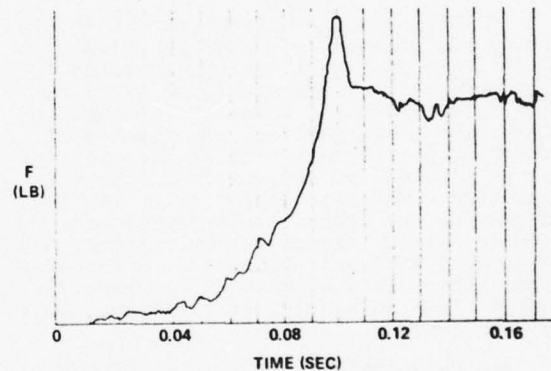


FIG. 5 TYPICAL FORCE-TIME SIGNATURE FOR THE ELLIPTICAL PARACHUTE UNDER INFINITE MASS CONDITIONS

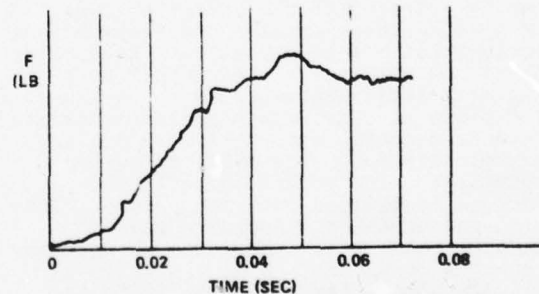


FIG. 6 TYPICAL FORCE-TIME SIGNATURE FOR THE RING SLOT PARACHUTE 20% GEOMETRIC POROSITY UNDER INFINITE MASS CONDITIONS

Infinite mass opening-shock signatures of several types of parachutes are presented in Figures 2 through 6. Analysis of these signatures using the force ratio, F/F_s , - time ratio, t/t_0 , technique indicated a similarity in the performance of the various solid cloth types of

parachutes which were examined. The geometrically porous ring slot parachute displayed a completely different signature, as was expected. These data are illustrated in Figure 7. If an initial boundary

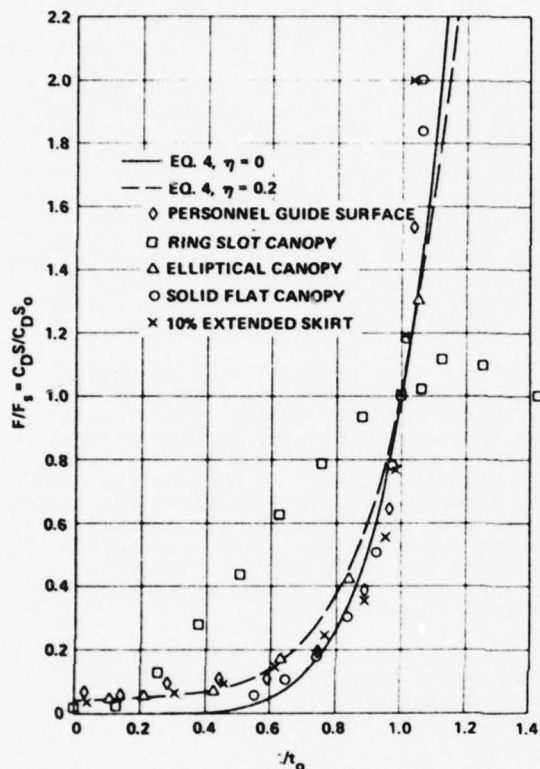


FIG. 7 DRAG AREA RATIO VS. TIME RATIO

condition of $C_D S / C_{D0} S_0 = 0$ at time $t/t_0 = 0$ is assumed, then, the data can be approximated by fitting a curve of the form

$$\frac{C_D S}{C_{D0} S_0} = \left(\frac{t}{t_0}\right)^6 \quad (3)$$

A more realistic drag area ratio expression was determined which includes the effect of initial area at line stretch.

$$\frac{C_D S}{C_{D0} S_0} = \left[\left(1 - \eta\right) \left(\frac{t}{t_0}\right)^3 + \eta \right]^2 \quad (4)$$

where η is the ratio of the projected mouth area at line stretch to the steady-state projected frontal area. Expanding equation (4)

$$\frac{C_D S}{C_{D0} S_0} = \left(1 - \eta\right)^2 \left(\frac{t}{t_0}\right)^6 + 2\eta \left(1 - \eta\right) \left(\frac{t}{t_0}\right)^3 + \eta^2 \quad (5)$$

At the time that equation (5) was ascertained, it suggested that the geometry of the deploying parachute was independent of density and velocity. It was also postulated that although this expression had been determined for the infinite mass condition, it would also be true for the finite mass case. This phenomenon has since been independently observed and confirmed by Berndt and De Weese in reference (2).

Since the drag area ratio was determined from actual parachute deployments, it was assumed that the effects of apparent mass and included mass on the deployment force history were accommodated.

The right-hand term of equation (2) contains the expression

$$\frac{2W}{\rho g V_s t_0 C_{D0} S_0} = M \quad (6)$$

This term can be visualized as shown in Figure 8 to be a ratio of the retarded mass (including the parachute) to an associated mass of atmosphere contained in a right circular cylinder which is generated by moving an inflated parachute of area $C_{D0} S_0$ for a distance equal to the product of $V_s t_0$ through an atmosphere of density, ρ .

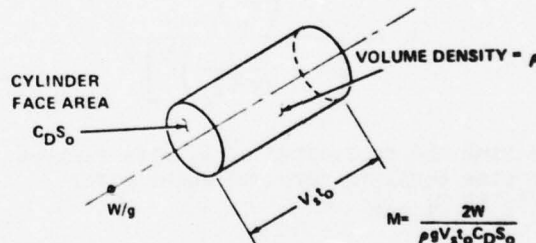


FIG. 8 VISUALIZATION OF THE MASS RATIO CONCEPT

The mass ratio, M , is the scale factor which controls the velocity and force profiles during parachute deployment. Substituting M and $C_D S / C_{D0} S_0$ into equation (2), integrating, and solving for V/V_s

$$\frac{V}{V_s} = \frac{1}{1 + \frac{1}{M} \left[\frac{(1 - \eta)^2}{7} \left(\frac{t}{t_0}\right)^7 + \frac{\eta(1 - \eta)}{2} \left(\frac{t}{t_0}\right)^4 + \eta^2 \frac{t}{t_0} \right]} \quad (7)$$

The instantaneous shock factor is defined as

$$x_1 = \frac{F}{F_s} = \frac{\frac{1}{2} \rho v^2 C_D S}{\frac{1}{2} \rho v_s^2 C_D S_o}$$

If the altitude variation during deployment is small, then, the density may be considered as constant

$$x_1 = \frac{C_D S}{C_D S_o} \left(\frac{v}{v_s} \right)^2$$

from equations (5) and (7)

$$x_1 = \frac{(1-\eta)^2 \left(\frac{t}{t_o} \right)^6 + 2\eta(1-\eta) \left(\frac{t}{t_o} \right)^3 + \eta^2}{\left[1 + \frac{1}{M} \left[\frac{(1-\eta)^2}{7} \left(\frac{t}{t_o} \right)^7 + \frac{\eta(1-\eta)}{2} \left(\frac{t}{t_o} \right)^4 + \eta^2 \frac{t}{t_o} \right] \right]^2} \quad (8)$$

III. Maximum Shock Force and Time of Occurrence During the Unfolding Phase

The time of occurrence of the maximum instantaneous shock factor, x_1 , is difficult to determine for the general case. However, for $\eta = 0$, the maximum shock factor and time of occurrence are readily calculated. For $\eta = 0$

$$x_1 = \frac{\left(\frac{t}{t_o} \right)^6}{\left[1 + \frac{1}{7M} \left(\frac{t}{t_o} \right)^7 \right]^2}$$

Setting the derivative of x_1 with respect to time equal to zero and solving for t/t_o at x_1 max

$$\left(\frac{t}{t_o} \right) @ x_1 \text{ max} = \left(\frac{21M}{4} \right)^{\frac{1}{7}} \quad (9)$$

and the maximum shock factor is

$$x_1 \text{ max} = \frac{16}{49} \left(\frac{21M}{4} \right)^{\frac{6}{7}} \quad (10)$$

Equations (9) and (10) are valid for values of $M \leq \frac{4}{21}$ (0.19), since for larger values of M , the maximum shock force occurs in the elastic phase of inflation.

Figures 9 and 10 illustrate the velocity and force profiles generated from equations (7) and (8) for initial projected area ratios of $\eta = 0$, and 0.2 with various mass ratios.

IV. Methods for Calculation of the Reference Time, t_o

The ratio concept is an ideal method to analyze the effects of the various parameters on the velocity and force profiles of the opening parachutes; however, a means of calculating t_o is required before specific values can be computed. Methods for computing the varying mass flow into the inflating canopy mouth, the varying mass flow out through the varying inflated canopy surface area, and the volume of air, V_o , which must be collected during the inflation process are required.

Figure 11 represents a solid cloth-type parachute canopy at some instant during inflation. At any given instant, the parachute drag area is proportional to the maximum inflated diameter. Also, the maximum diameter in conjunction with the suspension lines determines the inflow mouth area (A-A) and the pressurized canopy area (B-B-B). This observation provided the basis for the following assumptions. The actual canopy shape is of minor importance.

a. The ratio of the instantaneous mouth inlet area to the steady-state mouth area is in the same ratio as the instantaneous drag area.

$$\frac{A_M}{A_{Mo}} = \frac{C_D S}{C_D S_o}$$

b. The ratio of the instantaneous pressurized cloth surface area to the canopy surface area is in the same ratio as the instantaneous drag area.

$$\frac{S}{S_o} = \frac{C_D S}{C_D S_o}$$

c. Since the suspension lines in the unpressurized area of the canopy are straight, a pressure differential has not developed, and, therefore, the net airflow in this zone is zero.

Based on the foregoing assumptions, the mass flow equation can be written

$$dm = m \text{ inflow} - m \text{ outflow}$$

$$\rho \frac{dV}{dt} = \rho V A_M - \rho A_S P$$

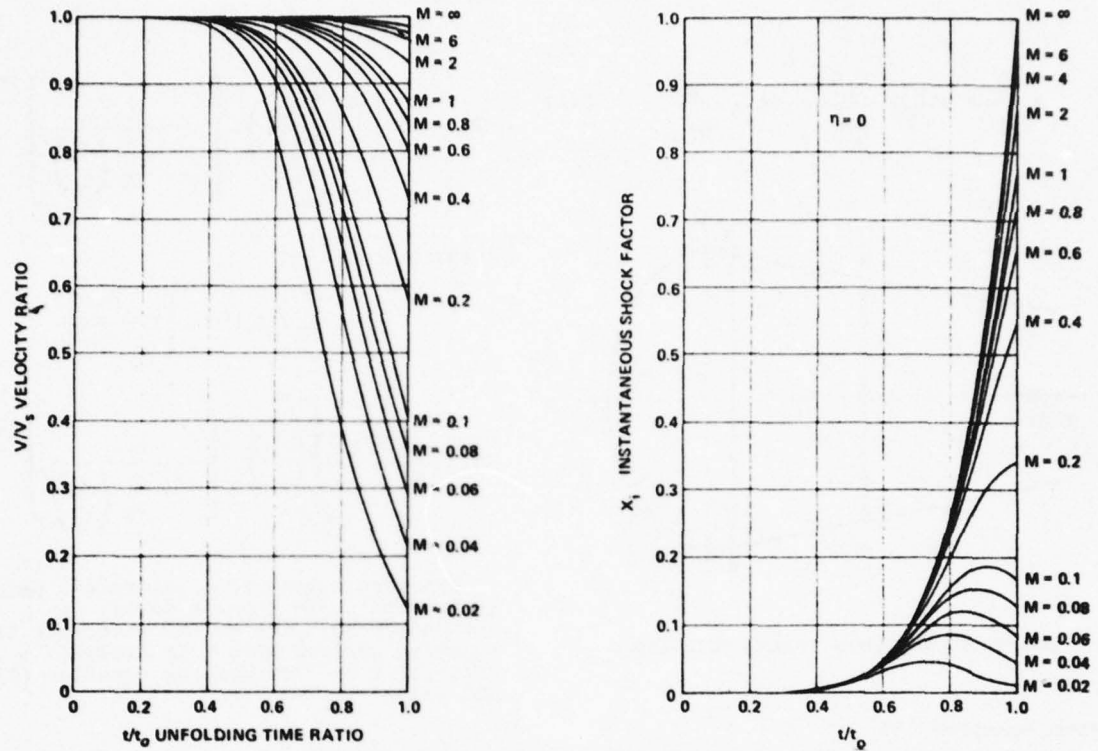


FIG. 9 EFFECT OF INITIAL AREA AND MASS RATIO ON THE SHOCK FACTOR AND VELOCITY RATIO DURING THE UNFOLDING PHASE FOR $\eta = 0$.

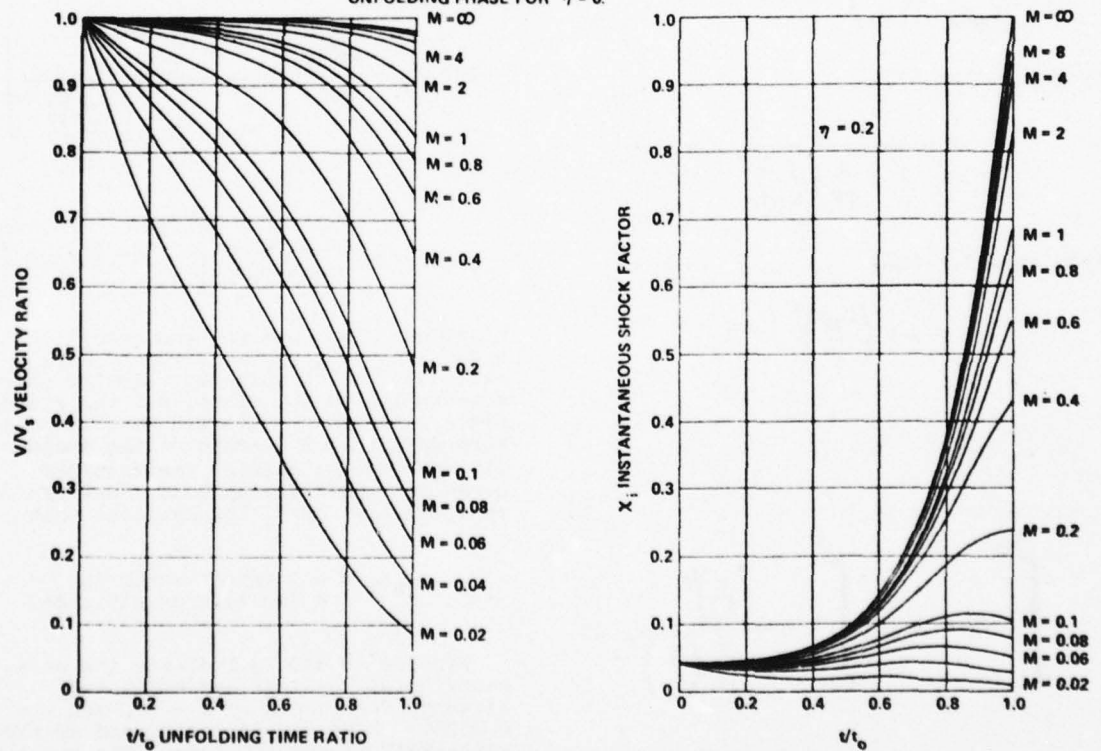


FIG. 10 EFFECT OF INITIAL AREA AND MASS RATIO ON THE SHOCK FACTOR AND VELOCITY RATIO DURING THE UNFOLDING PHASE FOR $\eta = 0.2$.

$$\rho \frac{dV}{dt} = \rho V A_{Mo} \frac{C_D S}{C_{DS_o}} - \rho A_{So} \frac{C_D S}{C_{DS_o}} P \quad (11)$$

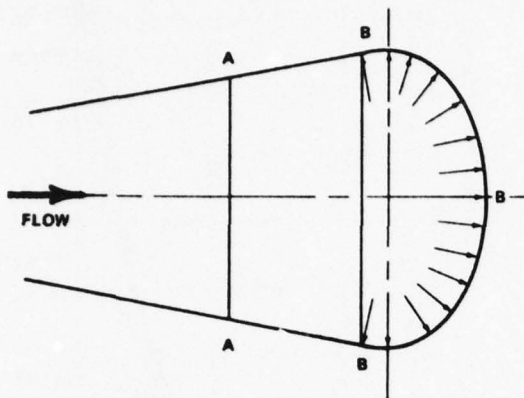


FIG. 11 PARTIALLY INFLATED PARACHUTE CANOPY

From equation (3)

$$\frac{C_D S}{C_{DS_o}} = \left(\frac{t}{t_o} \right)^6 ; \text{ for } \eta = 0$$

From equation (7)

$$V = \frac{V_s}{1 + \frac{1}{7M} \left(\frac{t}{t_o} \right)^7} ; \eta = 0$$

From equation (26)

$$P = k \left(\frac{C_F \rho}{2} \right)^n V^{2n}$$

$$\int_0^{V_o} dV = A_{Mo} V_s \int_0^{t_o} \frac{\left(\frac{t}{t_o} \right)^6}{1 + \frac{1}{7M} \left(\frac{t}{t_o} \right)^7} dt$$

$$-A_{So} k \left(\frac{C_F \rho}{2} \right)^n \int_0^{t_o} \left(\frac{t}{t_o} \right)^6 \left[\frac{V_s}{1 + \frac{1}{7M} \left(\frac{t}{t_o} \right)^7} \right]^{2n} dt \quad (12)$$

Integrating:

$$V_o = A_{Mo} V_s t_o^M \ln \left[1 + \frac{1}{7M} \right]$$

$$-A_{So} k \left(\frac{C_F \rho}{2} \right)^n \int_0^{t_o} \left(\frac{t}{t_o} \right)^6 \left[\frac{V_s}{1 + \frac{1}{7M} \left(\frac{t}{t_o} \right)^7} \right]^{2n} dt \quad (13)$$

Measured values of n indicate a data range from 0.574 through 0.771. A convenient solution to the reference time equation evolves when n is assigned a value of $1/2$. Integrating equation (13) and using

$$V_s t_o^M = \frac{2W}{g \rho C_{DS_o}}$$

$$\text{LET } K_1 = \frac{g \rho V_o}{2W} \left[\frac{C_{DS_o}}{A_{Mo} - A_{So} k \left(\frac{C_F \rho}{2} \right)^{1/2}} \right]$$

$$t_o = \frac{14W}{g \rho V_s C_{DS_o}} \left[e^{K_1} - 1 \right] \quad (14)$$

Equation (14) expresses the unfolding reference time, t_o , in terms of mass, altitude, snatch velocity, airflow characteristics of the cloth, and the steady-state parachute geometry. Note that the term $g \rho V_o / W$ is the ratio of the included air mass to the mass of the retarded hardware. Multiplying both sides of equation (14) by V_s demonstrates that

$$V_s t_o = \text{a constant which is a function of altitude}$$

Figures 12 and 13 indicate the parachute unfolding time and unfolding distance for values of $n = 1/2$ and $n = 0.63246$. Note the variation and convergence with rising altitude. The opening-shock force is strongly influenced by the inflation time. Because of this, the

value of t_0 calculated by using a realistic value of n should be used in the lower atmosphere.

As an example of this method of opening-shock analysis, let us examine the effect of altitude on the opening-shock force of a T-10-type parachute retarding a 200-pound weight from a snatch velocity of $V_s = 400$ feet per second at sea level. Conditions of constant velocity and constant dynamic pressure are investigated. The results are presented in Figure 14. At low altitudes, the opening-shock force is less than the steady-state drag force; however, as altitude rises, the opening shock eventually exceeds the steady-state drag force at some altitude. This trend is in agreement with field test observations.

V. Correction of t_0 for Initial Area Effects

The unfolding reference time, t_0 , calculated by the previous methods assumes that the parachute inflates from zero drag area. In reality, a parachute has a drag

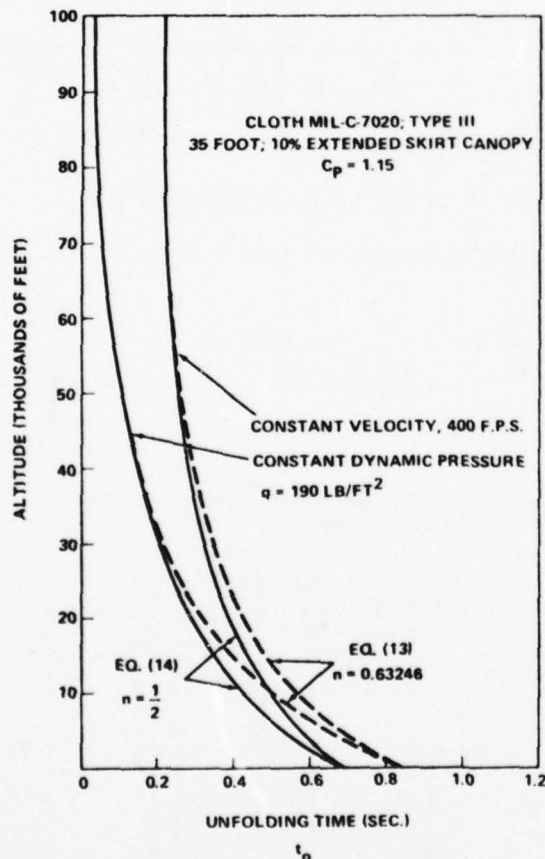


FIG. 12 EFFECT OF ALTITUDE ON THE UNFOLDING TIME " t_0 " AT CONSTANT VELOCITY AND CONSTANT DYNAMIC PRESSURE FOR $n = 1/2$ AND $n = 0.63296$

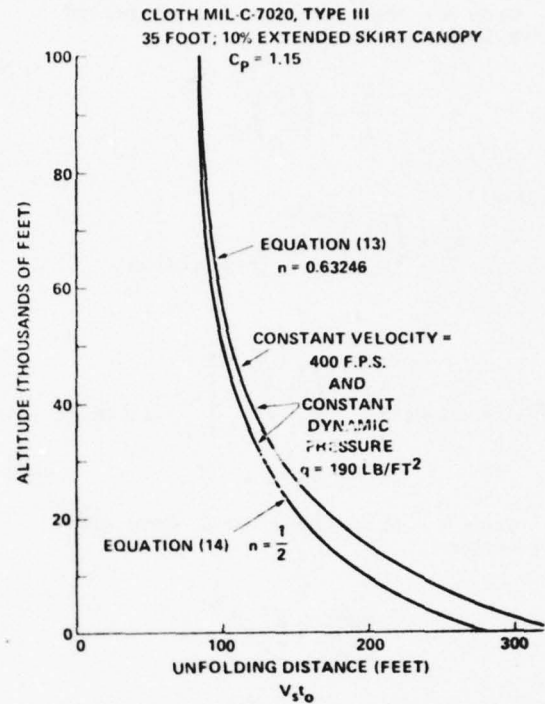


FIG. 13 EFFECT OF ALTITUDE ON THE UNFOLDING DISTANCE AT CONSTANT VELOCITY AND CONSTANT DYNAMIC PRESSURE FOR $n = 1/2$ AND $n = 0.63246$.

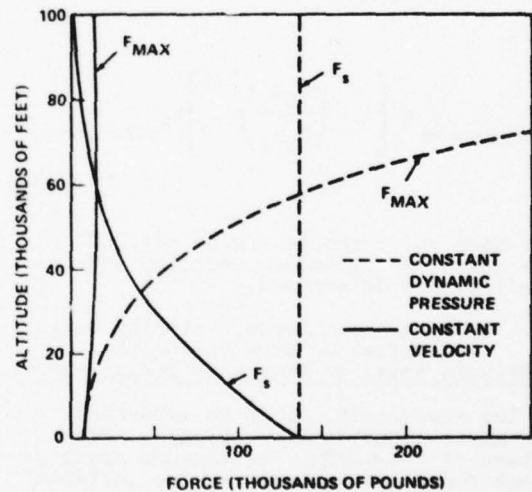


FIG. 14 VARIATION OF STEADY-STATE DRAG, F_s , AND MAXIMUM OPENING SHOCK WITH ALTITUDE FOR CONSTANT VELOCITY AND CONSTANT DYNAMIC PRESSURE

area at the beginning of inflation. Once t_0 has been calculated, a correction can be applied, based upon what is known about the initial conditions.

Case A - When the initial projected area is known

$$\frac{A_i}{A_c} = \left(\frac{t_i}{t_o}\right)^3$$

$$t_i = \left(\frac{A_i}{A_c}\right)^{1/3} t_{o\text{calculated}}$$

$$t_{o\text{corrected}} = \left[1 - \left(\frac{A_i}{A_c}\right)^{1/3}\right] t_{o\text{calculated}} \quad (15)$$

Case B - When the initial drag area is known

$$\frac{C_{DS_i}}{C_{DS_o}} = \left(\frac{t_i}{t_o}\right)^6$$

$$t_i = \left(\frac{C_{DS_i}}{C_{DS_o}}\right)^{1/6} t_{o\text{calculated}}$$

$$t_{o\text{corrected}} = \left[1 - \left(\frac{C_{DS_i}}{C_{DS_o}}\right)^{1/6}\right] t_{o\text{calculated}} \quad (16)$$

The mass ratio should now be adjusted for the corrected t_o before velocity and force profiles are determined.

VI. Opening-Shock Force, Velocity Ratio, and Inflation Time During the Elastic Phase of Parachute Inflation

The mass ratio, M , is an important parameter in parachute analysis. For values of $M \ll 4/21$, the maximum opening-shock force occurs early in the inflation process, and the elastic properties of the canopy are not significant. As the mass ratio approaches $M = 4/21$, the magnitude of the opening-shock force increases, and the time of occurrence happens later in the deployment sequence. For mass ratios $M > 4/21$, the maximum shock force will occur after the reference time, t_o . Parachutes designed for high mass ratio operation must provide a structure of sufficient constructed strength, F_c , so that the actual elongation of the canopy under load is less

than the maximum extensibility, ϵ_{max} , of the materials.

Development of the analysis in the elastic phase of inflation is similar to the technique used in the unfolding phase. Newton's second law of motion is used, together with the drag area ratio signature and mass ratio

$$\frac{C_{DS}}{C_{DS_o}} = \left(\frac{t}{t_o}\right)^6$$

which is still valid, as shown in Figure 7

$$\frac{1}{Mt_o} \int_{t_o}^t \left(\frac{t}{t_o}\right)^6 dt = v_s \int_{v_o}^v \frac{-dv}{v^2}$$

Integrating and solving for $\frac{v}{v_s}$

$$\frac{v}{v_s} = \frac{1}{\frac{v_s}{v_o} + \frac{1}{7M} \left[\left(\frac{t}{t_o}\right)^7 - 1 \right]} \quad (17)$$

where $\frac{v_o}{v_s}$ is the velocity ratio of the unfolding process at time $t = t_o$.

$$\frac{v_o}{v_s} = \frac{1}{1 + \frac{1}{M} \left[\frac{(1-\eta)^2}{7} + \frac{\eta(1-\eta)}{2} + \eta^2 \right]} \quad (18)$$

The instantaneous shock factor in the elastic phase becomes

$$x_i = \frac{C_{DS}}{C_{DS_o}} \left(\frac{v}{v_s}\right)^2$$

$$x_i = \frac{\left(\frac{t}{t_o}\right)^6}{\left[\frac{v_s}{v_o} + \frac{1}{7M} \left[\left(\frac{t}{t_o}\right)^7 - 1 \right] \right]^2} \quad (19)$$

The end point of the inflation process depends upon the applied loads, elasticity of the canopy, and the constructed strength of the parachute. A linear load elongation

relationship is utilized to determine the maximum drag area.

$$\frac{\epsilon}{F} = \frac{\epsilon_{\max}}{F_c}$$

$$\epsilon = \frac{F \epsilon_{\max}}{F_c} \quad (20)$$

The force, F , is initially the instantaneous force at the end of the unfolding process

$$F = X_o F_s \quad (21)$$

where X_o is the shock factor of the unfolding phase at $t = t_o$

$$X_o = \frac{1}{\left[1 + \frac{1}{M} \left[\frac{(1-\eta)^2}{7} + \frac{\eta(1-\eta)}{2} + \eta^2 \right] \right]^2} \quad (22)$$

Since the inflated shape is defined, the drag coefficient is considered to be constant, and the instantaneous force is proportional to the dynamic pressure and projected area. The maximum projected area would be developed if the dynamic pressure remained constant during the elastic phase. Under very high mass ratios, this is nearly the case over this very brief time period; but as the mass ratio decreases, the velocity decay has a more significant effect. The simplest approach for all mass ratios is to determine the maximum drag area of the canopy as if elastic inflation had occurred at constant dynamic pressure. Then utilizing the time ratio determined as an end point, intermediate shock factors can be calculated from equation (19) and maximum force assessed.

The initial force, $X_o F_s$, causes the canopy to increase in projected area. The new projected area in turn increases the total force on the canopy which produces a secondary projected area increase. The resulting series of events are resisted by the parachute materials. The parachute must, therefore, be constructed of sufficient strength to prevent the elongation of the materials from exceeding the maximum elongation.

$$\epsilon_o = \frac{X_o F_s}{F_c} \epsilon_{\max} \quad (23)$$

The next force in the series at constant q

$$F_1 = X_o F_s \frac{A_1}{A_c}$$

where

$$\frac{A_1}{A_c} = (1 + \epsilon_o)^2$$

Subsequent elongations in the system can be shown to be

$$\epsilon_1 = \epsilon_o (1 + \epsilon_o)^2$$

$$\epsilon_2 = \epsilon_o (1 + \epsilon_o (1 + \epsilon_o)^2)^2$$

The required canopy constructed strength can be determined for a given set of deployment conditions. The limiting value of the series (ϵ_t) determines the end point time ratio.

$$\left(\frac{t_f}{t_o} \right)^6 = \frac{C_{D S_{\max}}}{C_{D S_o}} = (1 + \epsilon_t)^2$$

$$\left(\frac{t_f}{t_o} \right) = \left(\frac{C_{D S_{\max}}}{C_{D S_o}} \right)^{1/6} = (1 + \epsilon_t)^{1/3} \quad (24)$$

Figure 15 illustrates the maximum drag area ratio as a function of ϵ_o .

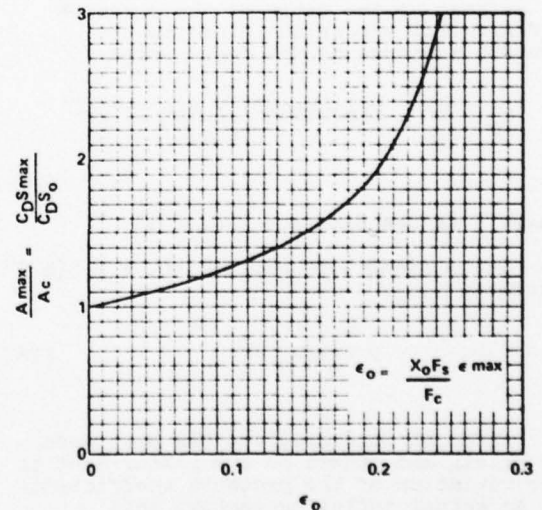


FIG. 15 MAXIMUM DRAG AREA RATIO VS. INITIAL ELONGATION

VII. Application of Cloth Permeability to the Calculation of the Inflation Time of Solid Cloth Parachutes

The mass outflow through the pressurized region of an inflating solid cloth parachute at any instant is dependent upon the canopy area which is subjected to airflow and the rate of airflow through that area. The variation of pressurized area as a function of reference time, t_0 , was earlier assumed to be proportional to the instantaneous drag area ratio, leaving the rate-of-airflow problem to solve. The permeability parameter of cloth was a natural choice for determining the rate of airflow through the cloth as a function of pressure differential across the cloth. Heretofore, these data have been more of a qualitative, rather than quantitative, value. A new method of analysis was developed wherein a generalized curve of the form $P = k(\Delta P)^n$ was fitted to cloth permeability data for a number of different cloths and gives surprisingly good agreement over the pressure differential range of available data. The pressure differential was then related to the trajectory conditions to give a generalized expression which can be used in the finite mass ratio range, as well as the infinite mass case. The permeability properties were transformed into a mass flow ratio, M' , which shows agreement with the effective porosity concept.

Measured and calculated permeability pressure data for several standard cloths are illustrated in Figure 16. This method has been applied to various types of cloth between the extremes of a highly permeable 3-momme silk to a relatively impervious parachute pack container cloth with reasonably good results, see Figure 17.

The canopy pressure coefficient, C_p , is defined as the ratio of the pressure differential across the cloth to the dynamic pressure of the free stream.

$$C_p = \frac{\Delta P}{q} = \frac{P(\text{internal}) - P(\text{external})}{1/2 \rho V^2} \quad (25)$$

where V is based on equation (7).

The permeability expression, $P = k(\Delta P)^n$ becomes

$$P = k(C_p \frac{\rho V^2}{2})^n \quad (26)$$

Although some progress has been made by Melzig and others on the measurement of the variation of the pressure coefficient on an actual inflating canopy, this dimension and its variation with time are still dark areas at the time of this writing. At the present time, a constant average value of pressure coefficient is

used in these calculations. Figure 18 presents the effect of pressure coefficient and altitude on the unfolding time for constant deployment conditions.

It is well known that the inflation time of solid cloth parachutes decreases as the operational altitude increases. This effect can be explained by considering the ratio of the mass outflow through a unit cloth area to the mass inflow through a unit mouth area.

$$M' = \text{mass flow ratio} = \frac{\text{mass outflow}}{\text{mass inflow}}$$

where

$$\text{mass outflow} = P \frac{\text{slugs}}{\text{ft}^2\text{-sec}} (\text{per ft}^2 \text{ cloth area})$$

and

$$\text{mass inflow} = V \frac{\text{slugs}}{\text{ft}^2\text{-sec}} (\text{per ft}^2 \text{ inflow area})$$

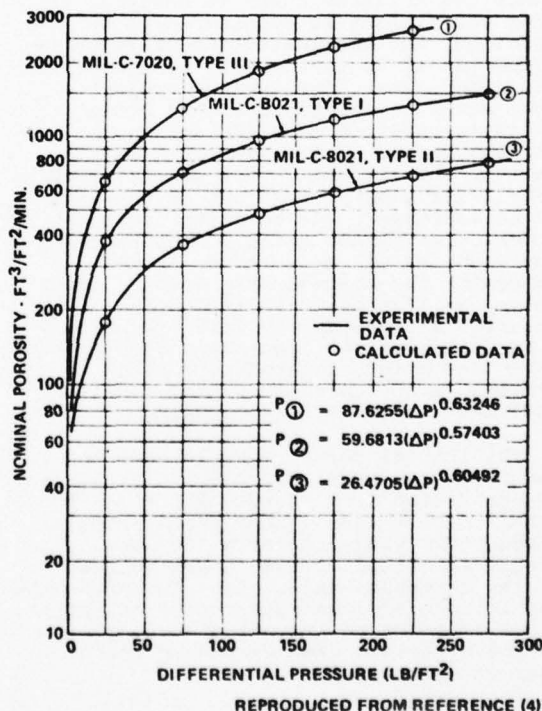


FIG. 16 NOMINAL POROSITY OF PARACHUTE MATERIAL VS DIFFERENTIAL PRESSURE.

Therefore, the mass flow ratio becomes

$$M' = \frac{P\rho}{V\rho} = \frac{P}{V}$$

$$M' = k \left(\frac{C_P \rho}{2} \right)^2 V^{(2n-1)} \quad (27)$$

Effective porosity, C , is defined as the ratio of the velocity through the cloth, u , to a fictitious theoretical velocity, v , which will produce the particular $\Delta P = 1/2 \rho v^2$.

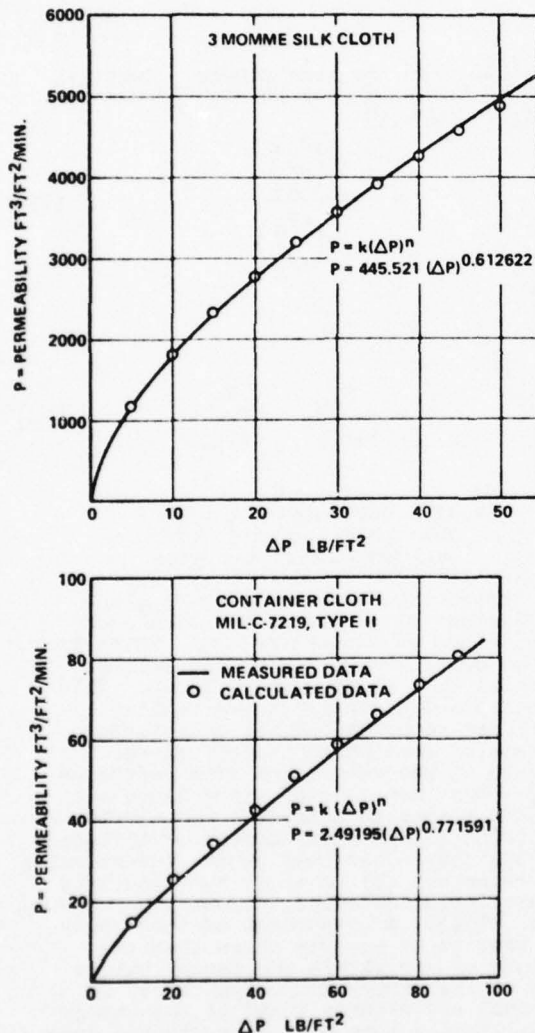


FIG. 17 COMPARISON OF MEASURED AND CALCULATED PERMEABILITY FOR RELATIVELY PERMEABLE AND IMPERMEABLE CLOTHS

AVERAGE CANOPY PRESSURE COEFFICIENT DURING INFLATION INCLUDING THE VENT

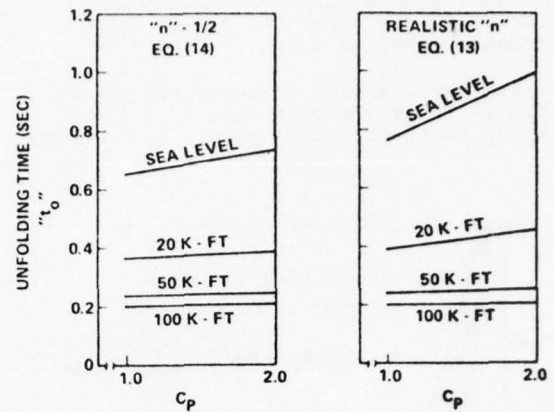


FIG. 18 EFFECT OF PRESSURE COEFFICIENT AND ALTITUDE ON THE UNFOLDING TIME.

$$\text{effective porosity, } C = \frac{u}{v} \quad (28)$$

Comparison of the mass flow ratio and previously published effective porosity data is shown in Figure 19. The effects of altitude and velocity on the mass flow ratio are presented in Figures 20, and 21 for constant velocity and constant altitude. The decrease of cloth permeability with altitude is evident.

The permeability constants " k " and " n ," can be determined from the permeability pressure differential data as obtained from an instrument such as a Frazier Permeameter. Two data points, "A" and

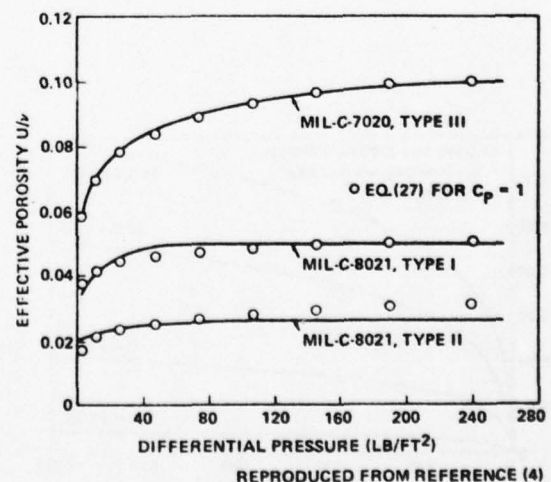


FIG. 19 THE EFFECTIVE POROSITY OF PARACHUTE MATERIALS VS. DIFFERENTIAL PRESSURE

"B," are selected in such a manner that point "A" is in a low-pressure zone below the knee of the curve, and point "B" is located in the upper end of the high-pressure zone, as shown in Figure 22.

The two standard measurements of 1/2 inch of water and 20 inches of water appear to be good data points if both are

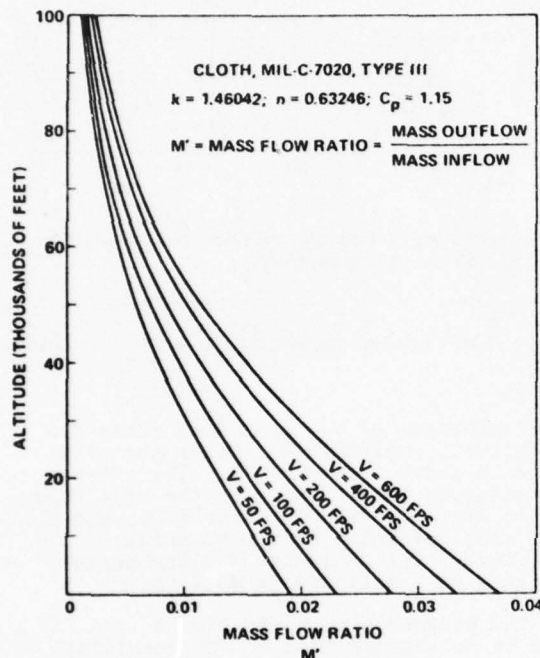


FIG. 20 EFFECT OF ALTITUDE ON MASS FLOW RATIO AT CONSTANT VELOCITY

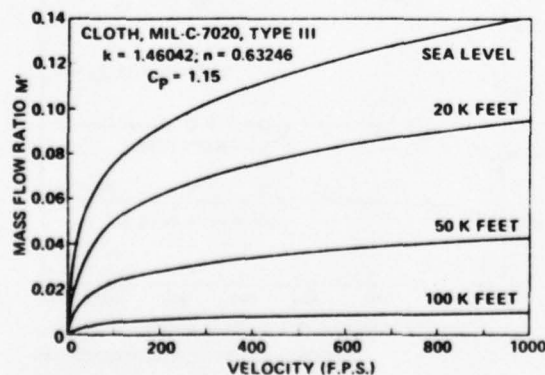


FIG. 21 EFFECT OF VELOCITY ON MASS FLOW RATIO AT CONSTANT DENSITY

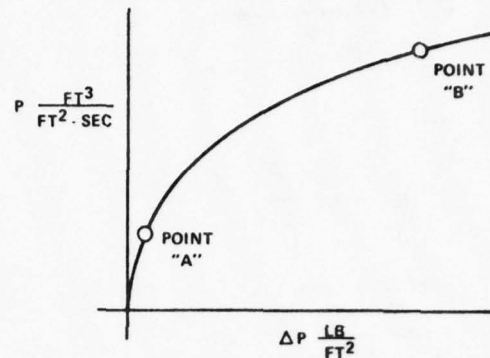


FIG. 22 LOCATION OF DATA POINTS FOR DETERMINATION OF "k" AND "n".

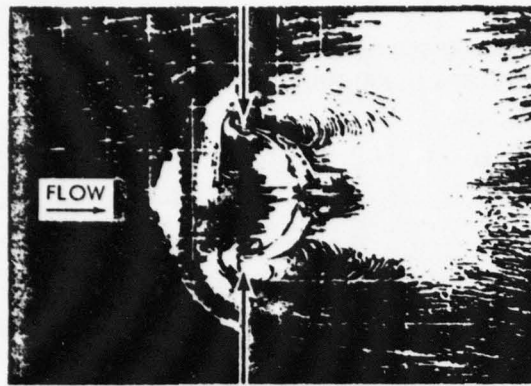
available on the same sample. Substituting the data from points "A" and "B" into $P = k(\Delta P)^n$:

$$n = \frac{\ln\left(\frac{P_B}{P_A}\right)}{\ln\left(\frac{\Delta P_B}{\Delta P_A}\right)} \quad (29)$$

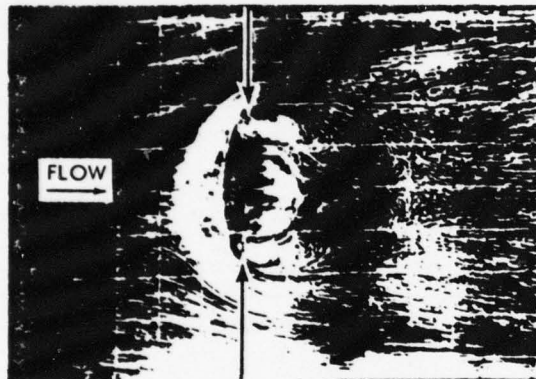
$$k = \frac{P_A}{(\Delta P_A)^n} = \frac{P_B}{(\Delta P_B)^n} \quad (30)$$

VIII. Determination of the Parachute Included Volume and Associated Air Mass

Before the reference time, t_0 , and inflation time, t_f , can be calculated, the volume of atmosphere, V_0 , which is to be collected during the inflation process must be accurately known. This requirement dictates that a realistic inflated canopy shape and associated volume of atmosphere be determined. Figure 23 was reproduced from reference (5). The technique of using lampblack coated plates to determine the airflow patterns around metal models of inflated canopy shapes was used by the investigator of reference (5) to study the stability characteristics of contemporary parachutes, i.e., 1943. A by-product of this study is that it is clearly shown that the volume of air within the canopy bulges out of the canopy mouth (indicated by arrows) and extends ahead of the canopy hem. This volume must be collected during the inflation process. Another neglected, but significant, source of canopy volume exists in the billowed portion of the gore panels.



HEMISPHERE



VENT PARACHUTE

REPRODUCED FROM REFERENCE (5)

FIG. 23 AIRFLOW PATTERNS SHOWING AIR VOLUME
AHEAD OF CANOPY HEM

The steady-state canopy shape has been observed in wind-tunnel and field tests to be elliptical in profile. Studies of the inflated shape and included volume of several parachute types (flat circular, 10 percent extended skirt, elliptical, hemispherical, ring slot, ribbon, and cross) are documented in references (6) and (7). These studies demonstrated that the steady-state profile shape of inflated canopies of the various types can be approximated to be two ellipses of common major diameter, $2\bar{a}$, and dissimilar minor diameters, b and b' , as shown in Figure 24. It was also shown that the volume of the ellipsoid of revolution formed by revolving the profile shape about the canopy axis was a good approximation of the volume of atmosphere to be collected during canopy inflation and included the air volume extended ahead of the parachute skirt hem together with the billowed gore volume.

$$\bar{V}_0 = \frac{2}{3} \pi \bar{a}^3 \left[\frac{b}{\bar{a}} + \frac{b'}{\bar{a}} \right] \quad (31)$$

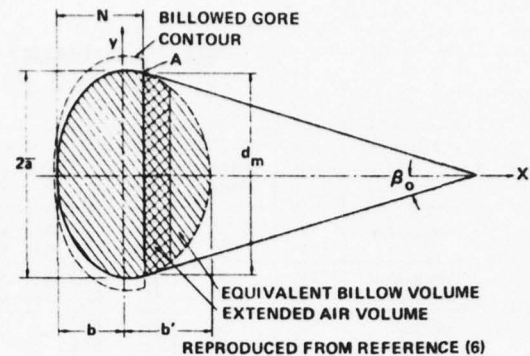


FIG. 24 PARACHUTE CROSS SECTION NOMENCLATURE

Tables I and II are summaries of test results reproduced from references (6) and (7), respectively, for the convenience of the reader.

IX. References

1. "A Method to Reduce Parachute Inflation Time with a Minor Increase in Opening Force," WADD Report TR 60-761
2. Berndt, R. J., and DeWesse, J. H., "Filling Time Prediction Approach for Solid Cloth Type Parachute Canopies," AIAA Aerodynamic Deceleration Systems Conference, Houston, Texas, 7-9 Sep 1966
3. "Theoretical Parachute Investigations," Progress Report No. 4, Project No. 5, WADC Contract AF33 (616)-3955, University of Minnesota
4. "Performance of and Design Criteria for Deployable Aerodynamic Decelerators," TR ASK-TR-61-579, AFFDL, AIRFORCESYSCOM, Dec 1963
5. "Investigation of Stability of Parachutes and Development of Stable Parachutes from Fabric of Normal Porosity," Count Zeppelin Research Institute Report No. 300, 23 Mar 1943
6. Ludtke, W. P., "A New Approach to the Determination of the Steady-State Inflated Shape and Included Volume of Several Parachute Types," NOLTR 69-159, 11 Sep 1969
7. Ludtke, W. P., "A New Approach to the Determination of the Steady-State Inflated Shape and Included Volume of Several Parachute Types in 24-Gore and 30-Gore Configurations," NOLTR 70-178, 3 Sep 1970

**TABLE I SUMMARY OF PARACHUTE SHAPE TEST RESULTS
FOR 12-GORE AND 16-GORE CONFIGURATIONS**

Parachute Type	No. of Gores	Suspension Line Length inches	Velocity		Scale Factor, K				$\frac{N}{a}$	Axes Ratio			Volume in ³			$\frac{V_o}{V_H}$
			mph	fps	$\frac{2\bar{a}}{D_o}$	$\frac{2\bar{a}}{D_F}$	$\frac{2\bar{a}}{D_R}$	$\frac{2\bar{a}}{L}$		$\frac{b}{a}$	$\frac{b'}{a}$	$\frac{b}{a} + \frac{b'}{a}$	V_H	V_C	V_o	
Flat Circular	12	34	50	73	.645	.650			.856	.6115	.8817	1.4932	4476	4481	6980	1.56
	16	34	50	73	.663	.669			.820	.5558	.9039	1.4597	4450	4100	7325	1.65
10% Extended Skirt	12	34	100	147	.663	.652			.881	.6424	.8860	1.5284	3928	4400	6783	1.73
	16	34	17	25	.654	.640			.785	.5580	.8502	1.4082	4051	3920	6197	1.53
Elliptical	12	34	75	110			.916		.812	.5626	.9657	1.5283		3322	5405	
	16	34	17	25			.875		.800	.6169	.8163	1.4332		2726	4405	
Hemispherical	12	34	125	183			.996		1.254	1.0005	.9080	1.9085		6224	8666	
	16	34	75	110			.994		1.185	.9129	.9380	1.8509		5921	8370	
Ringlot 16% Geometric Porosity	12	34	25	37	.607	.654			.853	.6566	.8735	1.530	3800	3650	5903	1.55
	12	34	100	147	.616	.663			.922	.6566	.8735	1.530	3800	4198	6166	1.62
	12	34	200	293	.637	.686			.918	.6566	.8735	1.530	3800	4624	6826	1.90
	16	34	25	37	.611	.658			.827	.6004	.8890	1.4894	3800	3763	5685	1.50
	16	34	100	147	.617	.664			.864	.6004	.8890	1.4894	3800	3985	6030	1.59
	16	34	200	293	.645	.695			.844	.6004	.8890	1.4894	3800	4430	6897	1.82
Ribbon 24% Geometric Porosity	12	34	25	37	.586	.632			.859	.6558	.8768	1.5326	3800	3323	5335	1.40
	12	34	100	147	.615	.663			.837	.6558	.8768	1.5326	3800	3714	6163	1.62
	12	34	200	293	.632	.681			.877	.6558	.8768	1.5326	3800	4280	6683	1.76
	16	34	25	37	.603	.650			.797	.5570	.8578	1.4148	3800	3438	5358	1.41
	16	34	100	147	.626	.674			.791	.5570	.8578	1.4148	3800	3804	5983	1.57
	16	34	200	293	.648	.698			.781	.5570	.8578	1.4148	3800	4164	6656	1.75
Cross Chute W/L = .264		34	25	37	.710			.543	1.242	.8867	1.2776	2.1643	1928	3768	5798	3.01
		34	100	147	.707			.540	1.270	.8867	1.2776	2.1643	1928	3810	5712	2.96
		34	200	293	.716			.547	1.285	.8867	1.2776	2.1643	1923	4212	5925	3.07
		47	25	37	.759			.580	1.113	.8494	1.2512	2.1006	1928	4052	6868	3.56
		47	100	147	.729			.557	1.205	.8494	1.2512	2.1006	1928	3973	5958	3.09
		47	200	293	.775			.592	1.110	.8494	1.2512	2.1006	1928	4292	7303	3.79

REPRODUCED FROM REFERENCE (6)

**TABLE II SUMMARY OF PARACHUTE SHAPE TEST RESULTS
FOR 24-GORE AND 30-GORE CONFIGURATIONS**

Parachute Type	No. of Gores	Suspension Line Length inches	Velocity		Scale Factor, K				$\frac{N}{a}$	Axes Ratio			Volume in ³			$\frac{V_o}{V_H}$
			mph	fps	$\frac{2\bar{a}}{D_o}$	$\frac{2\bar{a}}{D_F}$	$\frac{2\bar{a}}{D_R}$	$\frac{2\bar{a}}{L}$		$\frac{b}{a}$	$\frac{b'}{a}$	$\frac{b}{a} + \frac{b'}{a}$	V_H	V_C	V_o	
Flat Circulars	24	34	50	73	.677	.679			.795	.5758	.8126	1.3884	4362	4695	7273	1.67
	30	34	17	25	.668	.669			.827	.6214	.7806	1.4020	4342	4626	7027	1.62
10% Extended* Skirt	24	34	100	147	.665	.648			.834	.5949	.8771	1.4720	4138	4446	6930	1.67
	30	34	17	25	.650	.633			.825	.6255	.7962	1.4127	4172	4076	6265	1.50
Ring Slot 16% Geometrically Porous	24	34	25	37	.663	.665			.824	.5800	.9053	1.4853	3591	3878	5031	1.68
	24	34	100	147	.680	.682			.819	.5800	.9053	1.4853	3591	4079	6510	1.81
	24	34	200	293	.694	.696			.809	.5800	.9053	1.4853	3591	4270	6924	1.93
	30	34	25	37	.677	.678			.788	.5800	.9053	1.4853	3582	3826	6404	1.79
	30	34	100	147	.684	.685			.802	.5800	.9053	1.4853	3582	4023	6588	1.84
	30	34	200	293	.698	.699			.800	.5800	.9053	1.4853	3582	4260	7012	1.96
Ribbon 24% Geometrically Porous	24	34	25	37	.671	.673			.770	.5980	.8187	1.4167	3591	3591	5968	1.66
	24	34	100	147	.676	.678			.813	.5980	.8187	1.4167	3591	3927	6097	1.70
	24	34	200	293	.687	.689			.804	.5980	.8187	1.4167	3591	4061	6389	1.78
	30	34	25	37	.655	.657			.782	.6021	.8463	1.4484	3582	3396	5666	1.58
	30	34	100	147	.669	.670			.784	.6021	.8463	1.4484	3582	3622	6022	1.68
	30	34	200	293	.677	.679			.823	.6021	.8463	1.4484	3582	4002	6256	1.75

*Since this parachute was "breathing" during the test, several photographs were taken at each speed. The data were reduced from the photograph which most reasonably appeared to represent the equilibrium state.

REPRODUCED FROM REFERENCE (7)

X. List of Symbols

A_C	- Steady-state projected area of the inflated parachute, ft^2	P	- Cloth permeability - rate of air-flow through a cloth at an arbitrary differential pressure, $ft^3/ft^2 \text{ sec}$
A_M	- Instantaneous canopy mouth area, ft^2	q	- Dynamic pressure, lb/ft^2
A_{M0}	- Steady-state inflated mouth area, ft^2	S	- Instantaneous inflated canopy surface area, ft^2
a	- Acceleration, ft/sec^2	S_0	- Canopy surface area, ft^2
$2\bar{a}$	- Maximum inflated parachute diameter of gore mainseam, ft	t	- Instantaneous time, sec
b	- Minor axis of the ellipse bounded by the major axis ($2\bar{a}$) and the vent of the canopy, ft	t_0	- Reference time when the parachute has reached the design drag area for the first time, sec
b'	- Minor axis of the ellipse which includes the skirt hem of the canopy, ft	t_f	- Canopy inflation time when the inflated canopy has reached its maximum physical size, sec
C	- Effective porosity	u	- Air velocity through cloth in effective porosity, ft/sec
C_D	- Parachute coefficient of drag	v	- Fictitious theoretical velocity used in effective porosity, ft/sec
C_p	- Parachute pressure coefficient, relates internal and external pressure (ΔP) on canopy surface to the dynamic pressure of the free stream	\dot{V}	- Instantaneous system velocity, ft/sec
D_0	- Nominal diameter of the aerodynamic decelerator = $\sqrt{4S_0/\pi}$, ft	V_0	- System velocity at the time $t = t_0$, ft/sec
F	- Instantaneous force, lbs	V_s	- System velocity at the end of suspension line stretch, ft/sec
F_s	- Steady-state drag force that would be produced by a fully open parachute at velocity V_s , lbs	\bar{V}_0	- Volume of air which must be collected during the inflation process, ft^3
F_c	- Constructed strength of the parachute, lbs	W	- Hardware weight, lb
F_{max}	- Maximum opening-shock force, lbs	x_i	- Instantaneous shock factor
g	- Gravitational acceleration, ft/sec^2	X_0	- Shock factor at the time $t = t_0$
k	- Permeability constant of canopy cloth	ρ	- Air density, $slugs/ft^3$
m	- Mass, $slugs$	η	- Ratio of parachute projected mouth area at line stretch to the steady-state projected area
M	- Mass ratio - ratio of the mass of the retarded hardware (including parachute) to a mass of atmosphere contained in a right circular cylinder of length ($V_s t_0$), face area ($C_D S_0$), and density (ρ)	ϵ	- Instantaneous elongation
M'	- Mass flow ratio - ratio of atmosphere flowing through a unit cloth area to the atmosphere flowing through a unit inlet area at arbitrary pressure	ϵ_{max}	- Maximum elongation
n	- Permeability constant of canopy cloth	ϵ_0	- Initial elongation at the beginning of the elastic phase of inflation
		S.F.	- Parachute safety factor = F_c/F_{max}

Appendix C

A GUIDE FOR THE USE OF APPENDIX B

At first reading, Appendix B may appear to be a complicated system of analysis because of the many formulas presented. Actually, once understood, the technique is straightforward and uncomplicated. The author has attempted to simplify the algebra wherever possible. This appendix presents, in semi-outline form, a guide to the sequence of calculations because the analysis does require use of formulas from the text, not necessarily in the order in which they were presented. Also, the user can be referenced to graphs of performance to illustrate effects.

In order to compute t_0 , other parameters must be obtained from various sources.

I. Determine System Parameters

1. C_{DSO} , drag area, ft^2 obtained from design requirement.
2. V_S , fps, velocity of system at suspension line stretch.
3. ρ , slugs/ ft^3 , air density at deployment altitude.
4. W , lb, system weight (including weight of the parachute) from design requirements.
5. V_O , ft^3 , this volume of air, which is to be collected during inflation, is calculated from the steady-state inflated shape geometry of the particular parachute type. The nomenclature is described in Figure 24, p. B-13. When D_O or D_F is known, \bar{a} can be calculated from data in Table I and Table II, p. B-14, for various parachute types and number of gores. Then the geometric volume V_O can be calculated by Equation (31), p. B-13, with appropriate values of b/\bar{a} and b'/\bar{a} from the tables.

6. A_{MO} , ft^2 , steady-state canopy mouth area

$$A_{MO} = \pi \bar{a}^2 \left[1 - \left(\frac{N/\bar{a} - b/\bar{a}}{b'/\bar{a}} \right)^2 \right] \quad (C-1)$$

where n/\bar{a} , b/\bar{a} , and b'/\bar{a} are available from Tables I and II for the particular type of parachute and number of gores.

7. A_{SO} , ft^2 , canopy surface area = $\frac{\pi D_O^2}{4}$

8. C_p , pressure coefficient, see Figure 18, p. B-11. A constant $C_p = 1.7$ for all altitudes seems to yield acceptable results.

9. Constants k and n are derived from measurements of the air flow through the cloth. Only k is needed for Equation (14), but n is also required for Equation (13). These parameters can be determined for any cloth using the technique described beginning on p. B-11. The two-point method is adequate if the ΔP across the cloth is in the range of ΔP for actual operation. Check-points of cloth permeability can be measured and compared to calculated values to verify agreement. If the data is to be extrapolated to operational ΔP 's greater than measured, a better method of determining k and n from the test data would be a least squares fit through many data points. This way errors due to reading either of the two points are minimized.

II. Step 1

Calculate the reference time t_0 by use of Equations (13) or (14), p. B-6. If the deployment altitude is 50,000 feet or higher, Equation (14) is preferred due to its simplicity. For altitudes from sea level to 50,000 feet, Equation (13) is preferred. Figure 12, p. B-7, shows the effect of altitude on t_0 and can be taken as a guide for the user to decide whether to use Equation (13) or (14). One should keep in mind that the opening shock force can be a strong function of inflation time, so be as realistic as possible. If Equation (13) is elected, the method in use at the NSWC/WO is to program Equation (13) to compute the parachute volume, V_O , for an assumed value of t_0 . Equation (14), because of its simplicity, can be used for a first estimate of t_0 at all altitudes. The computed canopy volume is then compared to the canopy volume calculated from the geometry of the parachute as per Equation (31), p. B-13. If the volume computed from the mass flow is within the volume computed from the geometry within plus or minus a specified delta volume, the time t_0 is printed out. If not within the specified limits, t_0 is adjusted, and a new volume calculated. For a 35-foot D_O , T-10 type canopy, I use plus or minus 10 cubic feet in the volume comparison. The limit would be reduced for a parachute of smaller D_O .

If V_O calculated = V_O geometry ± 10 , then print answer.

If V_O calculated $\neq V_O$ geometry ± 10 , then correct t_0 as follows:

$$t_o = t_o \frac{V_O \text{ geometry}}{V_O \text{ calculated}} \quad (C-2)$$

The new value of t_0 is substituted in the "do loop" and the volume recomputed. This calculation continues until the required volume is within the specified limits.

III. Calculate t_0 corrected for initial area. The t_0 of Section II assumes that the parachute inflated from a zero initial area. If this is a reasonable assumption for the particular system under study, then the mass ratio can be determined from Equation (6), p. B-3. For $\eta = 0$ if the value of $M \leq 0.19$, then a finite state of deployment exists, and the time ratio of occurrence and the maximum shock factor can be determined from Equations (9) and (10) respectively on p. B-4. If $\eta \neq 0$, then the limiting mass ratio for finite operations will rise slightly as described in Appendix D. Figures D-1 and D-2 illustrate the effects of initial area on limiting mass ratios and shock factors respectively. If the mass ratio is greater than the limiting mass ratio (M_L), then the maximum shock force occurs at a time greater than t_0 and the elasticity of the materials must be considered (see Section IV).

If $\eta \neq 0$, then the reference time t_0 will be reduced, and the mass ratio will rise due to partial inflation at the line stretch. Figures 9 and 10, p. B-5, illustrate the effects of initial area on the velocities and shock factor during the "unfolding" inflation. Equation (15), p. B-8, can be used to correct t_0 calculated for where $\eta = A_i/A_c$. If the initial value of drag area is known, Equation (16), p. B-8, can be used to correct t_0 and rechecked for limiting mass ratios versus η in Appendix D.

IV. Opening shock calculations in the elastic phase of inflation. It has been considered that from time $t = 0$ to $t = t_0$ the parachute has been inelastic. At the time $t = t_0$ the applied aerodynamic load causes the materials to stretch and the parachute canopy increases in size. The increased size results in an increase in load, which causes further growth, etc. This sequence of events continues until the applied forces have been balanced by the strength of materials. The designer must insure that the constructed strength of the materials is sufficient to resist the applied loads for the material elongation expected. Use of materials of low elongation should result in lower opening shock forces as $C_D S_{max}$ is reduced.

When the mass ratio of the system is greater than the limiting mass ratio, the elasticity of the materials and material strength determine the maximum opening shock force. The maximum elongation ϵ_{max} and the ultimate strength of the materials are known from tests or specifications. The technique begins on p. B-8.

At the time $t = t_0$ calculate the following quantities for the particular values of M and η .

- a. V_0/V_s from Equation (18), p. B-8.

- b. X_0 from Equation (22), p. B-9.
- c. ϵ_0 from Equation (23), p. B-9.
- d. Determine $C_{DS_{max}}/C_{DS_0}$ from Figure 15, p. B-9.
- e. Calculate the inflation time ratio t_f/t_0 from Equation (24), p. B-9.
- f. Calculate the maximum shock factor from Equation (19), p. B-8.
- g. Calculate the opening shock force $F_{max.} = \chi_1 F_s$ where

$$F_s = \frac{1}{2} \rho V_s^2 C_D S_0$$

- h. Calculate filling time, t_f (sec)

$$\chi = t_0 \left(\frac{t_f}{t_0} \right)$$

V. In order to simplify the required effort, the work sheets of Table C-1 are included on pages C-5 through C-9 to aid the engineer in systematizing the analysis. The work sheets should be reproduced to provide additional copies.

Table C-1. Opening Shock Force

CALCULATION WORK SHEETS

	SYMBOL	VALUE	DIMENSION
1. Parachute type -			
2. System parameters			
a. System weight, W (lb)		W	lb.
b. Gravity, g (ft/sec ²)		g	ft/sec ²
c. Deployment altitude (ft)			ft.
d. Deployment air density, ρ (slugs/ft ³)		ρ	slugs/ft ³
e. Velocity at line stretch, V_s (fps)		V_s	fps.
f. Steady state canopy data			
(1) Diameter, D_o (ft)		D_o	ft.
(2) Inflated diameter, $2\bar{a}$ (ft); $\frac{2\bar{a}}{D_o} = *$		$2\bar{a}$	ft.
(3) Surface area, S_o (ft ²); $\frac{\pi}{4} D_o^2$		S_o	ft.
(4) Drag area, $C_D S_o$ (ft ²); $C_D \times S_o$		$S_D S_o$	ft. ²
(5) Mouth area, A_{MO}^* (ft)			
$A_{MO} = \pi \bar{a}^2 \left[1 - \left(\frac{N/\bar{a} - b/\bar{a}}{b'/\bar{a}} \right)^2 \right]$		A_{MO}	ft. ²
(6) Volume, V_o^* (ft ³)			
$V_o = \frac{2}{3} \pi \bar{a}^3 \left[\frac{b}{\bar{a}} + \frac{b'}{\bar{a}} \right]$		V_o	ft. ³
g. Cloth data			
(1) K } Calculate using technique beginning on		K	
(2) n } p. B-11. Note: Permeability is usually measured as ft ³ /ft ² /min. For these calculations permeability must be expressed as ft ³ /ft ² /sec		n	

* Data for these calculations are listed in Tables 1 and 2, p. B-14.

Table C-1. Opening Shock Force
(cont'd)

(3) ϵ_{\max} ; determine maximum elongations from pull test data of joints, seams, lines, etc. Use minimum ϵ_{\max} determined from tests.

(4) C_p ; pressure coefficient

h. Steady state drag, F_s (lb) = $F_s = \frac{1}{2} \rho V_s^2 C_D S_o$

i. Parachute constructed strength, F_c (lb); determined from data on efficiency of seams, joints, lines. Constructed strength is the minimum load required to fail a member times the number of members.

3. Force calculations

a. Calculate t_o for $\eta = 0$; eq. 14, p. B-6.

$$t_o = \frac{14W}{\rho g V_s C_D S_o} \left[\epsilon \frac{\frac{\rho g V_o}{2W} \left[\frac{C_D S_o}{A_{MO} - A_{SO} K \left(\frac{C_p \rho}{2} \right)^{\frac{1}{2}}} \right]}{-1} \right]$$

Check Figure 12, p. B-7 for advisability of using eq. 13, p. B-6.

b. If $\eta = 0$, proceed with steps c through e. If $\eta \neq 0$, go to step f.

c. Mass ratio, M ; eq. 6, p. B-3

$$M = \frac{2W}{\rho g V_s t_o C_D S_o}$$

d. If $M \leq 4/21$ for $\eta = 0$, then finite mass deployment is indicated.

(1) Time ratio at $x_{i \max}$; eq. 9, p. B-4

$$\frac{t}{t_o @ x_{i \max}} = \left(\frac{21M}{4} \right)^{\frac{1}{7}}$$

(2) Max shock factor, x_i ; eq., 10, p. B-4

$$x_{i \max} = \frac{16}{49} \left(\frac{21M}{4} \right)^{\frac{6}{7}}$$

SYMBOL	VALUE	DIMENSION
C_p		
F_s		lb.
F_c		lb
t_o		sec.
M		-
$\frac{t}{t_o @ x_{i \max}}$		-
$x_{i \max}$		-

Table C-1. Opening Shock Force
(Cont'd)

- (3) Max shock force,
- F_{\max}
- (lb)

$$F_{\max} = X_{i \max} F_s$$

e. If $M > 4/21$; then intermediate mass or infinite mass deployment is indicated and the elasticity of materials is involved. Calculate the trajectory conditions at time $t = t_o$.

- (1) Velocity ratio @
- $t = t_o$
- for
- $\eta = 0$

$$\frac{V_o}{V_s} = \frac{1}{1 + \frac{1}{7M}}$$

- (2) Shock factor
- X_o
- @
- $t = t_o$
- for
- $\eta = 0$

$$X_o = \frac{1}{\left[1 + \frac{1}{7M}\right]^2} = \left(\frac{V_o}{V_s}\right)^2$$

- (3) Initial elongation,
- ϵ_o
- ; eq. 23, p. B-9

$$\epsilon_o = \frac{X_o F_s}{F_c} \epsilon_{\max}$$

- (4) Determine
- $\frac{C_D S_{\max}}{C_D S_o}$
- from Figure 15, p. B-9

- (5) Calculate inflation time ratio,
- $\frac{t_f}{t_o}$
- ; eq. 24, p. B-9

$$\frac{t_f}{t_o} = \left(\frac{C_D S_{\max}}{C_D S_o}\right)^{\frac{1}{6}}$$

- (6) Calculate maximum shock factor,
- $x_{i \max}$
- ; eq. 19, p. B-8

$$X_{i \max} = \frac{\left(\frac{t_f}{t_o}\right)^6}{\left[\frac{V_s}{V_o} + \frac{1}{7M} \left[\left(\frac{t_f}{t_o}\right)^7 - 1\right]\right]^2}$$

- (7) Calculate maximum shock force,
- F_{\max}
- (lb),

$$F_{\max} = X_{i \max} F_s$$

SYMBOL	VALUE	DIMENSION
	F_{\max}	lb.
	$\frac{V}{V_o}$	-
	X_o	-
	ϵ_o	-
	$\frac{C_D S_{\max}}{C_D S_o}$	-
	$\frac{t_f}{t_o}$	-
	$X_{i \max}$	-
	F_{\max}	lb.

Table C-1. Opening Shock Force
(cont'd)

SYMBOL	VALUE	DIMENSION
(8) Inflation time, sec = $t_f = t_0 \left(\frac{t_f}{t_0} \right)$	t_f	Sec.
f. If $\eta \neq 0$, correct t_0 for initial area effects; eq. 16, p. B-8	$t_0 = \left[1 - \left(\frac{C_D S_i}{C_D S_o} \right)^{1/6} \right]$ to calculated	Sec.
g. Mass Ratio, M, eq. 6, p. B-3		
$M = \frac{2W}{\rho g V_s t_0 C_D S_o}$		
h. Calculate limiting mass ratio, M_L ; eq. D-2, p. D-2		
$M_L = \frac{1}{3(1-\eta)} - \left[\frac{9}{14} \eta^2 + \frac{3}{14} \eta + \frac{1}{7} \right]$	M_L	-
If $M \leq M_L$, finite mass deployment is indicated and x_i max can be determined by eq. 8, p. B-4 by assuming values of t/t_0 and plotting the data using the methods of Appendix D.		
i. If $M > M_L$, then intermediate mass or infinite mass deployment is indicated and the elasticity of materials is involved. Calculate the trajectory conditions at time $t = t_0$.		
(1) Velocity ratio @ $t = t_0$ for $\eta \neq 0$; eq. 18, p. B-8		
$\frac{v_o}{v_s} = \frac{1}{\left[1 + \frac{1}{M} \left[\frac{(1-\eta)^2}{7} + \frac{\eta(1-\eta)}{2} + \eta^2 \right] \right]}$	$\frac{v_o}{v_s}$	-
(2) Shock factor X_o @ $t = t_0$ for $\eta \neq 0$; eq. 22, p. B-9		
$X_o = \frac{1}{\left[1 + \frac{1}{M} \left[\frac{(1-\eta)^2}{7} + \frac{\eta(1-\eta)}{2} + \eta^2 \right] \right]^2} = \left(\frac{v_o}{v_s} \right)^2$	X_o	-
(3) Initial elongation, ϵ_o ; eq. 23, p. B-9		
$\epsilon_o = \frac{X_o F_s}{F_e} \epsilon_{max}$	ϵ_o	-
(4) Determine $\frac{C_D S_{max}}{C_D S_o}$ from Figure 15, p. B-9	$\frac{C_D S_{max}}{C_D S_o}$	-

Table C-1. Opening Shock Force (Contd.)

p. B-9	SYMBOL	VALUE	DIMENSION
(5) Calculate inflation time ratio, $\frac{t_f}{t_o}$; eq. 24,	$\frac{t_f}{t_o} = \left(\frac{C_D S_{max}}{C_D S_o} \right)^{\frac{1}{6}}$	$\frac{t_f}{t_o}$	—
(6) Calculate maximum shock factor, $x_{i \max}$; eq. 19, p. B-8	$x_{i \max} = \frac{\left(\frac{t_f}{t_o} \right)^6}{\left[\frac{V_s}{V_o} + \frac{1}{7M} \left[\left(\frac{t_f}{t_o} \right)^7 - 1 \right] \right]^2}$	$x_{i \max}$	—
(7) Calculate maximum shock force, F_{\max} (lb)	$F_{\max} = x_{i \max} F_s$	F_{\max}	lb.
(8) Calculate inflation time, t_f (sec)	$t_f = t_o \left(\frac{t_f}{t_o} \right)$	t_f	Sec.

Appendix D

EFFECT OF INITIAL AREA RATIO ON THE LIMITING MASS RATIO
AND SHOCK FACTOR FOR THE FINITE STATE OF
SOLID CLOTH PARACHUTE DEPLOYMENT

Very low mass ratios are indicative of finite mass parachute deployment, wherein the maximum shock force occurs before the parachute is fully inflated during the unfolding phase of deployment. As the mass ratio is increased, the maximum shock force occurs later in the inflation process. At some value of mass ratio, the maximum shock force will occur at the time t_0 . This particular mass ratio is defined as the limiting mass ratio (M_L) for finite mass deployment. A further increase in mass ratio will result in the maximum shock force occurring after the parachute has achieved the design drag area ($C_D S_0$) for the first time.

Equation (8), from p. 4, Appendix B, defines the instantaneous shock factor during the unfolding phase of parachute deployment.

$$x_i = \frac{(1-\eta)^2 \left(\frac{t}{t_0}\right)^6 + 2\eta(1-\eta) \left(\frac{t}{t_0}\right)^3 + \eta^2}{\left[1 + \frac{1}{M} \left[\frac{(1-\eta)^2}{7} \left(\frac{t}{t_0}\right)^7 + \frac{\eta(1-\eta)}{2} \left(\frac{t}{t_0}\right)^4 + \eta \frac{t}{t_0} \right] \right]^2}$$

This expression is to be analyzed for the following purposes:

- a. Determine the effect of the initial area ratio (η) on the limiting mass ratio (M_L).
- b. Determine the variations of the instantaneous shock factor during the unfolding phase of deployment as a function of limiting mass ratio and η .
- c. Determine the expression for the time of occurrence of the maximum shock force for finite mass ratios less than the limiting mass ratio.

The maximum shock force occurs at the point in finite mass deployment where $dx_i/dt = 0$. Setting the derivative $dx_i/dt = 0$ and solving for mass ratio as a function of η and t/t_0 results in the following equality:

$$M = \frac{\left[(1-\eta)^2 \left(\frac{t}{t_0} \right)^6 + 2\eta(1-\eta) \left(\frac{t}{t_0} \right)^3 + \eta^2 \right]^2}{3 \left[(1-\eta)^2 \left(\frac{t}{t_0} \right)^5 + \eta(1-\eta) \left(\frac{t}{t_0} \right)^2 \right]} - \left[\frac{(1-\eta)^2}{7} \left(\frac{t}{t_0} \right)^7 + \frac{\eta(1-\eta)}{2} \left(\frac{t}{t_0} \right)^4 + \eta^2 \frac{t}{t_0} \right] \quad (D-1)$$

Since the limiting mass ratio occurs at $t/t_0 = 1$, Equation (D-1) can be reduced to:

$$M_L = \frac{1}{3(1-\eta)} - \left[\frac{9}{14} \eta^2 + \frac{3}{14} \eta + \frac{1}{7} \right] \quad (D-2)$$

The effects of initial area ratio on the limiting mass ratio are described in Equation (D-2) and Figure D-1. Note that the time of occurrence of the maximum shock force for $\eta = 0$ in Equation (D-1) is:

$$\frac{t}{t_0} \otimes x_{i_{\max}} = \left(\frac{21M}{4} \right)^{\frac{1}{7}} \quad (D-3)$$

which is the same as Equation (9), p. 4, Appendix B.

The variation of the instantaneous shock factor during the unfolding phase of deployment for limiting mass ratios is presented in Figure D-2. Initial area at the beginning of inflation causes the initial force to increase, but this is compensated for by reduced maximum shock forces. As η increases, the initial loads can be greater than the maximum shock force. However, values of η are usually small and depend on the deployment systems for magnitude and repeatability. Values of $\eta = 0.4$ are more representative of a parachute being disreefed rather than initially deployed. This does demonstrate, however, that the analysis presented in Appendix B can be adapted to the disreefing of solid cloth parachutes by considering the next stage to be a deployment with a large value of η . Variation in initial area is one of the causes of variation in opening shock forces. The variation of opening shock forces for finite mass, intermediate mass, and infinite mass states of deployment can be evaluated by successive calculations with various expected values of η .

For known mass ratios less than the limiting mass ratio, the time of occurrence of the maximum shock force can be ascertained from Equation D-1. If η approaches zero, then the time ratio of

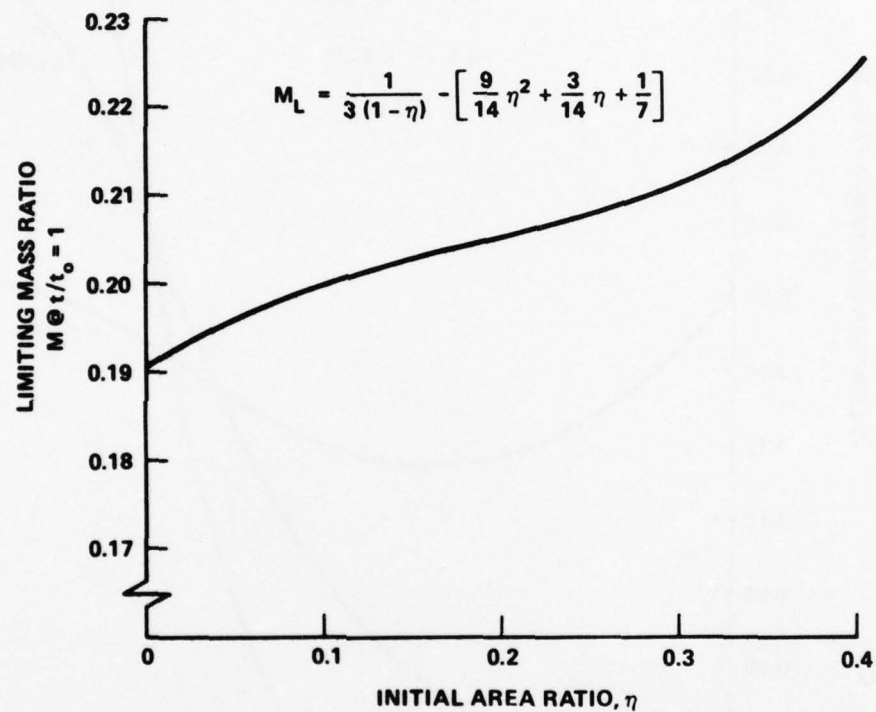


FIGURE D-1 EFFECT OF INITIAL AREA RATIO ON THE LIMITING MASS RATIO FOR THE FINITE STATE OF PARACHUTE DEPLOYMENT FOR SOLID CLOTH PARACHUTES

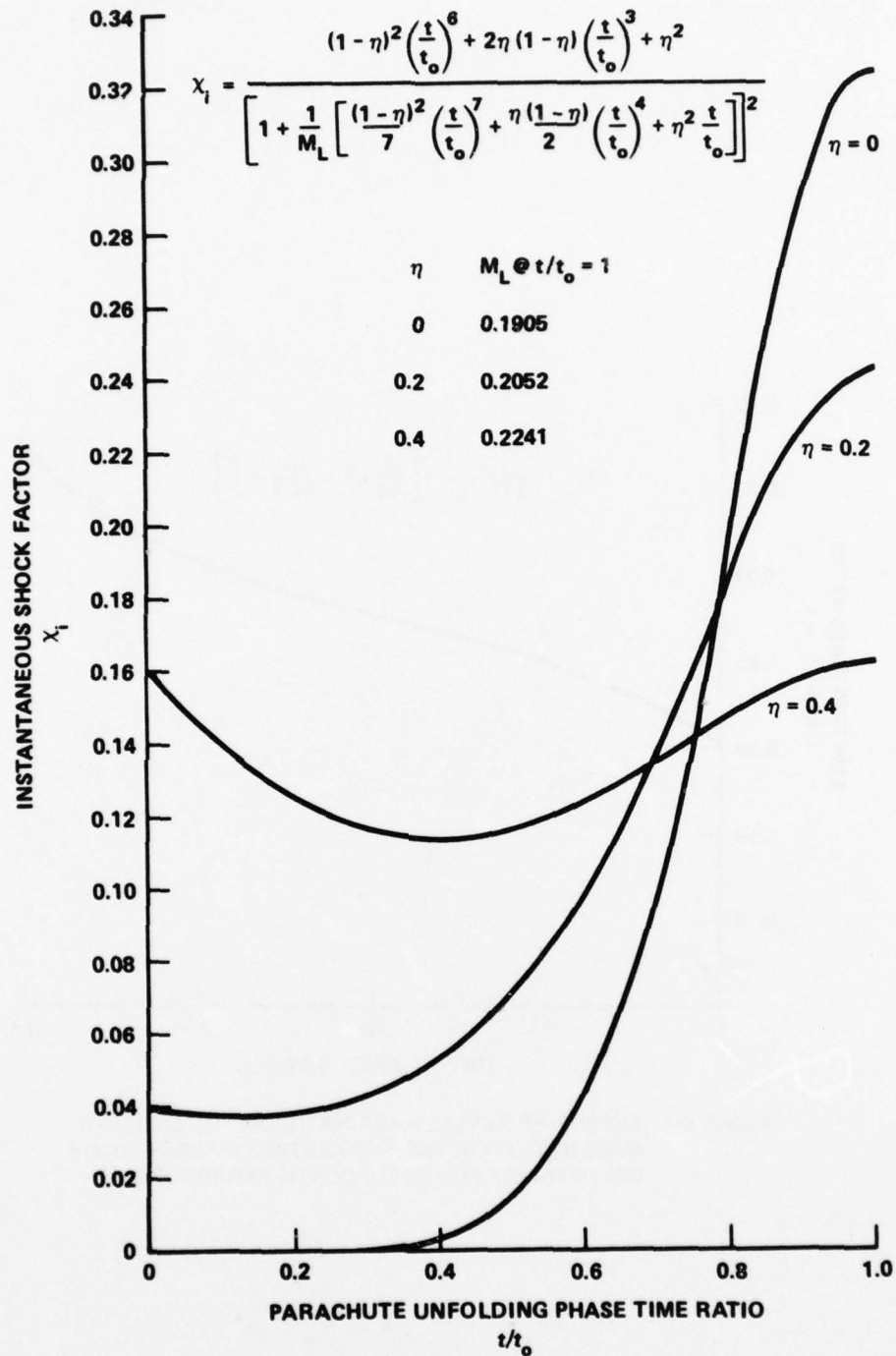


FIGURE D-2 VARIATION OF THE FINITE MASS SHOCK FACTOR DURING THE UNFOLDING PHASE OF SOLID CLOTH PARACHUTES FOR LIMITING MASS RATIOS AND INITIAL AREA EFFECTS

occurrence of the maximum shock force can be initially estimated from Equation (D-3), or determined by plotting

$$x_i = f M, \eta, \frac{t}{t_0}$$

as in Figure D-2.

SYMBOLS

- A_C - Steady-state projected area of the inflated parachute, ft^2
- A_i - Projected area at line stretch, ft^2
- A_M - Instantaneous canopy mouth area, ft^2
- A_{Mo} - Steady-state inflated mouth area, ft^2
- a - Acceleration, ft/sec^2
- $2\bar{a}$ - Maximum inflated parachute diameter of gore mainseam, ft
- b - Minor axis of the ellipse bounded by the major axis ($2\bar{a}$) and the vent of the canopy, ft
- b' - Minor axis of the ellipse which includes the skirt hem of the canopy, ft
- c - Speed of sound at analysis altitude, fps
- C - Effective porosity
- C_D - Parachute coefficient of drag
- $C_D S_0$ - Steady state parachute drag area, ft^2
- C_p - Parachute pressure coefficient, relates internal and external pressure (ΔP) on canopy surface to the dynamic pressure of the free stream

- D_A - Aerodynamic diameter, ft
- D_O - Nominal diameter of the aerodynamic decelerator = $\sqrt{4S_O/\pi}$, ft
- F_R - Froude number
- F - Instantaneous force, lbs
- F_S - Steady-state drag force that would be produced by a fully open parachute at velocity V_s , lbs
- F_C - Constructed strength of the parachute, lbs
- F_{max} - Maximum opening-shock force, lbs
- g - Gravitational acceleration, ft/sec²
- k - Permeability constant of canopy cloth
- m - Mass, slugs
- M - Mass ratio - ratio of the mass of the retarded hardware (including parachute) to a mass of atmosphere contained in a right circular cylinder of length ($V_s t_O$), face area ($C_D S_O$), and density (ρ)
- M' - Mass flow ratio - ratio of atmosphere flowing through a unit cloth area to the atmosphere flowing through a unit inlet area at arbitrary pressure
- M_n - Mach number
- n - Permeability constant of canopy cloth
- P - Cloth permeability - rate of airflow through a cloth at an arbitrary differential pressure, ft³/ft² sec

- q - Dynamic pressure, lb/ft^2
- R_e - Reynolds number
- S - Instantaneous inflated canopy surface area, ft^2
- S_o - Canopy surface area, ft^2
- t - Instantaneous time, sec
- t_o - Reference time when the parachute has reached the design drag area for the first time, sec
- t_f - Canopy inflation time when the inflated canopy has reached its maximum physical size, sec
- u - Air velocity through cloth in effective porosity, ft/sec
- v - Fictitious theoretical velocity used in effective porosity, ft/sec
- V - Instantaneous system velocity, ft/sec
- V_o - System velocity at the time $t = t_o$, ft/sec
- V_s - System velocity at the end of suspension line stretch, ft/sec
- \underline{V}_o - Volume of air which must be collected during the inflation process, ft^3
- W - Hardware weight, lb
- x_i - Instantaneous shock factor
- X_o - Shock factor at the time $t = t_o$
- ρ - Air density, slugs/ft^3

- η - Ratio of parachute projected mouth area at line stretch to the steady-state projected area

- ϵ - Instantaneous elongation

- ϵ_{\max} - Maximum elongation

- ϵ_0 - Initial elongation at the beginning of the elastic phase of inflation

- S.F. - Parachute safety factor = F_c/F_{\max}

- μ - Dynamic viscosity, $\frac{\text{lb-sec}}{\text{ft}^2}$

GLOSSARY OF TERMS

Aerodynamic diameter. Preference length used in the computation of Reynold's number and Froude number.

$$D_A = \sqrt{C_D S_0}$$

Aerodynamic size. Name for steady-state parachute drag area, $C_D S_0$.

Ballistic coefficient. Ratio of retarded weight to parachute steady-state drag area, $W/C_D S_0$.

Elastic phase of inflation. Inflation time from $t_0 < t \leq t_f$ when the elasticity of parachute materials are resisting opening shock force.

Finite mass state of operation. Maximum shock force occurs before complete inflation at time $t=t_0$.

Intermediate mass state of operation. Maximum shock force occurs after the parachute has opened to its steady-state drag area for the first time. The mass ratio $M_L < M < 10$. At low mass ratios maximum force can be much lower than infinite mass calculations.

Limiting mass ratio. The highest mass ratio for finite mass state of operation. Maximum shock occurs at $t=t_0$.

State of parachute operation. Relates to time of occurrence of the opening shock force and is a function of $\left(M, \eta, \frac{t}{t_0}\right)$.

Unfolding phase of inflation. Inflation time from $0 \leq t \leq t_0$ when the canopy is inflating.

DISTRIBUTION

Commander
Naval Air Systems Command
Attn: AIR-3032B
AIR-5203
AIR-5301
AIR-5302
Department of the Navy
Washington, DC 20361

Commander
Naval Sea Systems Command
Attn: SEA-03A
SEA-035
SEA-05A
SEA-05121
SEA-0521
SEA-054
SEA-9132
Department of the Navy
Washington, DC 20362

2

Commanding Officer
U.S. Army Mobility Equipment Research
and Development Center
Attn: Technical Document Center
Fort Belvoir, VA 22060

Commander
David W. Taylor Naval Ship Research & Development Center
Attn: Library
Code 581
Bethesda, MD 20034

Commander
U.S. Naval Missile Center
Attn: Technical Library
Point Mugu, CA 93041

Commander
Naval Weapons Center
Attn: Technical Library
China Lake, CA 93555

Commander
Naval Ocean Systems Center
San Diego, CA 92152

Commanding Officer
U.S. Naval Air Development Center
Attn: NADC Library
Warminster, PA 18974

Commanding Officer
Harry Diamond Laboratories
Attn: Technical Library
2800 Powder Mill Road
Adelphi, MD 20783

Office of Naval Research
Attn: Fluid Dynamics Branch
Structural Mechanics Branch
800 N. Quincy St.
Arlington, VA 22217

U.S. Army Ballistic Research Laboratories
Attn: Technical Library, Bldg. 313
Aberdeen Proving Ground, MD 21005

Defense Documentation Center
Cameron Station
Alexandria, VA 22314

12

Defense Advanced Research Projects Agency
Attn: Technical Library
1400 Wilson Boulevard
Arlington, VA 22209

Director
Defense Research and Engineering
Attn: Technical Library (3C-128)
Department of Defense
Washington, DC 20301

National Aeronautics and Space Administration
Wallops Station
Attn: Mr. Mendle Silbert
Wallops Island, VA 23336

National Aeronautics and Space Administration
Lewis Research Center
Attn: Technical Library
21000 Brookpark Road
Cleveland, OH 44135

National Aeronautics and Space Administration
Goddard Space Flight Center
Attn: Library
Greenbelt, MD 20771

Superintendent
U.S. Naval Postgraduate School
Attn: Library (Code 0384)
Monterey, CA 93940

Superintendent
U.S. Naval Academy
Attn: Library
Annapolis MD 21402

Sandia Corporation
Attn: Mr. William B. Pepper
Mr. R. C. Maydew
Dr. B. W. Roberts
Albuquerque, NM 87115

Sandia Corporation
Livermore Laboratory
Attn: Technical Reference Library
P. O. Box 969
Livermore, CA 94551

Lockheed Missiles and Space Company
Attn: Mr. K. French
P.O. Box 504
Sunnyvale, CA 94086

Rockwell International Corporation
Space and Information Systems Division
Attn: Technical Information Center
12214 S. Lakewood Boulevard
Downey, CA 90241

PA State University
Applied Research Laboratory
P. O. Box 30
State College, PA 16801

Honeywell, Incorporated
Attn: Mr. S. Sopczak
600 Second Street N.
Hopkins, MN 55343

University of Maryland
Mechanical Engineering Department
Attn: Professor A. Wiley Sherwood
College Park, MD 20742

University of Minnesota
Department of Aeronautical Engineering
Attn: Dr. Helmut Heinrich
Minneapolis, MN 55455

National Aeronautics and Space Administration
George C. Marshall Space Flight Center
Attn: Technical Library
Huntsville, AL 35812

National Aeronautics and Space Administration
Langley Research Center
Attn: Library, MS 185, Mr. Harold N. Morrow
Langley Station
Hampton, VA 23365

National Aeronautics and Space Administration
Ames Research Center
Attn: Technical Library
Moffett Field, CA 94035

National Aeronautics and Space Administration
Attn: Dr. H. H. Kurzweg, Director of Research
600 Independence Avenue, SW
Washington, DC 20546

Commanding Officer
Naval Research Laboratory
Attn: Code 2027
Library, Code 2029 (ONRL)
Washington, DC 20375

National Academy of Sciences
National Research Council
Committee on Undersea Warfare
2101 Constitution Avenue, NW
Washington, DC 20418

Commanding Officer
Naval Aerospace Recovery Facility
Attn: Mr. Howard C. Fish (Technical Director)
Naval Air Facility
El Centro, CA 92244

2

Commanding Officer
Air Force Flight Dynamics Laboratory
Wright-Patterson Air Force Base
Attn: Mr. Ralph Speelman
Mr. Oscar W. Sepp
Dayton, OH 45433

Applied Physics Laboratory
The Johns Hopkins University
Attn: Document Librarian
Johns Hopkins Road
Laurel, MD 20810

6

TO AID IN UPDATING THE DISTRIBUTION LIST
FOR NAVAL SURFACE WEAPONS CENTER, WHITE
OAK TECHNICAL REPORTS PLEASE COMPLETE THE
FORM BELOW:

TO ALL HOLDERS OF NSWC/WOL/TR 78-189
by William P. Ludtke, Code U-11

DO NOT RETURN THIS FORM IF ALL INFORMATION IS CURRENT

A. FACILITY NAME AND ADDRESS (OLD) (Show Zip Code)

NEW ADDRESS (Show Zip Code)

B. ATTENTION LINE ADDRESSES:

C.

☐ REMOVE THIS FACILITY FROM THE DISTRIBUTION LIST FOR TECHNICAL REPORTS ON THIS SUBJECT.

D.

NUMBER OF COPIES DESIRED